Generalized Distributions of Host Dispersion Measures in the Fast Radio Burst Cosmology

Jing-Yi Jia [a,*], Da-Chun Qiang [b], Lin-Yu Li [a], Hao Wei [a,†]

[a)] *School of Physics, Beijing Institute of Technology, Beijing 100081, China*

[b)] *Institute for Gravitational Wave Astronomy, Henan Academy of Sciences, Zhengzhou 450046, Henan, China*

ABSTRACT

As is well known, Hubble tension is one of the most serious challenges in cosmology to date. So, it is of interest to measure the Hubble constant by using some new probes independent of cosmic microwave background (CMB) and type Ia supernovae (SNIa). One of the promising probes is the fast radio bursts (FRBs), which could be useful in cosmology. In the literature, the methodology proposed by Macquart *et al.* has been widely used, in which both $\mathrm{DM_{IGM}}$ and $\mathrm{DM_{host}}$ are described by probability distribution functions. Recently, it was found that in order to obtain a Hubble constant H_0 consistent with the ones of Planck 2018 and SH0ES by using the current $\mathcal{O}(100)$ localized FRBs, an unusually large $f_{\rm IGM}$ fairly close to its upper bound 1 is required, if the narrow prior bounded by 0.5 for the parameter F in the distribution of $\mathrm{DM_{IGM}}$ was used. In fact, a small F is the key to make H_0 larger. In the present work, we consider a loose prior for the parameter F, and find an unusually low H_0 by using 125 localized FRBs. We show that the model with loose F prior is strongly preferred over the one with narrow F prior in all terms of the Bayesian evidence and the information criteria AIC, BIC. So, the great Hubble tension between FRBs, Planck 2018 and SH0ES should be taken seriously. Instead of modifying $\sigma_\Delta = Fz^{-0.5}$ in the distribution of $\mathrm{DM_{IGM}}$, here we try to find a new way out by generalizing the distribution of $\mathrm{DM_{host}}$ with varying location and scale parameters ℓ and e^μ, respectively. We find that H_0 can be consistent with the ones of Planck 2018 and SH0ES in all cases. All the Bayesian evidence and the information criteria AIC, BIC for the generalized distributions of $\mathrm{DM_{host}}$ are overwhelmingly strong.

PACS numbers: 98.80.Es, 98.70.Dk, 98.80.-k

[*] email address: jjy@bit.edu.cn

[†] Corresponding author; email address: haowei@bit.edu.cn

I. INTRODUCTION

As is well known, Hubble tension is one of the most serious challenges in cosmology to date [1–3]. In particular, the Hubble constant inferred from the final Planck measurements (Planck 2018) of the cosmic microwave background (CMB) in the early universe is given by $H_0 = 67.36 \pm 0.54$ km/s/Mpc [4]. On the other hand, the local determination of H_0 based on the Cepheid/Type Ia supernova (SNIa) distance ladder from the Hubble Space Telescope (HST) and the SH0ES team is given by $H_0 = 73.04 \pm 1.04$ km/s/Mpc [5]. There is a serious tension (beyond 5σ) between them. Many efforts have been made in the literature, but this significant discrepancy has not been well reconciled by now [1–3].

Obviously, it is of interest to measure the Hubble constant by using some new probes independent of CMB and SNIa. One of the promising probes is the fast radio bursts (FRBs) [6–13], which are mysterious transient radio sources of millisecond duration. Since almost all of FRBs are at extragalactic/cosmological distances (the inferred redshifts of FRBs could be $z \sim 3$ or even larger), they are useful to study cosmology and the intergalactic medium (IGM).

One of the key observational quantities of FRBs is dispersion measure (DM), namely the column density of the free electrons, due to the ionized medium (plasma) along the path. The observed DM of FRB at redshift z can be separated into [14–26]

$$\mathrm{DM_{obs}} = \mathrm{DM_{MW,\,ISM}} + \mathrm{DM_{MW,\,halo}} + \mathrm{DM_{IGM}} + \mathrm{DM_{host}}/(1+z)\,, \tag{1}$$

where $\mathrm{DM_{MW,\,ISM}}$, $\mathrm{DM_{MW,\,halo}}$, $\mathrm{DM_{IGM}}$, and $\mathrm{DM_{host}}$ are the contributions from the interstellar medium (ISM) and halo of our Milky Way (MW), IGM, and the host galaxy (including ISM of the host galaxy and the near-source plasma), respectively. In particular, $\mathrm{DM_{IGM}}$ records the main information about IGM and the cosmic expansion. The mean of $\mathrm{DM_{IGM}}$ at redshift z is given by [14–23]

$$\langle \mathrm{DM_{IGM}} \rangle = \frac{3cH_0\Omega_b}{8\pi G m_p} \int_0^z \frac{f_{\mathrm{IGM}}(\tilde{z})\, f_e(\tilde{z})\,(1+\tilde{z})\, d\tilde{z}}{E(\tilde{z})}\,, \tag{2}$$

where c is the speed of light, H_0 is the Hubble constant, Ω_b is the present fractional density of baryons, G is the gravitational constant, m_p is the mass of proton, $E(z) \equiv H(z)/H_0$ is the dimensionless Hubble parameter, $f_{\mathrm{IGM}}(z)$ is the fraction of baryon mass in IGM, and $f_e(z)$ is the ionized electron number fraction per baryon. In principle, one can constrain the cosmological parameters, especially the Hubble constant H_0, by using the observational data of FRBs.

In the FRB cosmology, DM plays the role of a proxy of the luminosity distance d_L. To study cosmology, the redshift of FRB should be known, but this is not easy. In the early years, cosmology has been studied by using the simulated FRBs with mock redshifts (see e.g. [14–23]). It is worth noting that the method of dark sirens in the field of gravitational waves was proposed to be applied to unlocalized FRBs in [27]. In the recent years, more and more FRBs have been well localized and hence their redshifts were observationally known. So, the FRB cosmology becomes thriving with these localized FRBs.

In the past years, $\mathrm{DM_{host}}$ was usually assumed to be a given constant, and $\langle \mathrm{DM_{IGM}} \rangle$ was directly used in place of $\mathrm{DM_{IGM}}$. However, these deviate from the real universe in fact. Noting that $\langle \mathrm{DM_{IGM}} \rangle$ is the mean value of $\mathrm{DM_{IGM}}$ in all directions of the lines of sight, and Eq. (2) is derived from cosmological principle, $\mathrm{DM_{IGM}}$ should deviate from $\langle \mathrm{DM_{IGM}} \rangle$ since the plasma density fluctuates along the line of sight [28–31]. Recently, the new methodology proposed by Macquart *et al.* [32] has been widely used in the literature. In this methodology, both $\mathrm{DM_{IGM}}$ and $\mathrm{DM_{host}}$ are instead described by probability distribution functions (PDFs), and the model parameters are constrained by maximizing the likelihood. We will briefly review this methodology in Sec. II A.

This Macquart's methodology works well in many cases of few localized FRBs. For instance, in [32], $\Omega_b h_{70}$ was well constrained by using only 8 localized FRBs, where $h_{70} = H_0/(70$ km/s/Mpc$)$. In e.g. [33], $H_0 = 68.81^{+4.99}_{-4.33}$ km/s/Mpc was found by using 18 localized FRBs, and it is consistent with both the SH0ES and Planck 2018 results. When the number of localized FRBs increased, the situation changed slowly. In e.g. [34], $H_0 \simeq 73 \sim 76$ km/s/Mpc was found by using 64 localized FRBs, and it is consistent with the SH0ES result but inconsistent with the one of Planck 2018. Very recently, when the number of localized FRBs became $\mathcal{O}(100)$, something made subtle difference. In e.g. [35], in order to get a Hubble constant $H_0 = 69.40^{+2.14}_{-1.97}$ km/s/Mpc consistent with the Planck 2018 result by using 108 localized FRBs, $f_{\mathrm{IGM}} = 0.93$ should be adopted, which is much larger than the traditional $f_{\mathrm{IGM}} = 0.82 \sim 0.84$ extensively used in the literature (e.g. [14–23]). In e.g. [36], adopting the SH0ES result $H_0 = 73.04 \pm 1.04$ km/s/Mpc, an unusual $f_{\rm IGM} = 0.999$ was found by using 107 localized FRBs, which is extremely close to its upper bound 1. To date, the debate on H_0 and $f_{\rm IGM}$ from localized FRBs is still not settled.

On the other hand, another point is about $\sigma_\Delta = Fz^{-0.5}$ in the Macquart's methodology (see Sec. II for details). In [32], a narrow prior $[\,0.011,\, 0.5\,]$ for the parameter F was suggested, where the upper bound is only 0.5. Actually, F cannot be constrained from the right hand side (see Extended Data Fig. 5 of [32]) by using 8 localized FRBs. But this is not due to the sparsity of data. As shown in e.g. Fig. 5 of [37], F still cannot be constrained from the right hand side even by using 115 localized FRBs. In fact, if the prior for F could be relaxed to e.g. $[\,0.01,\, 10.0\,]$, F can be well constrained, but a much larger $F \sim \mathcal{O}(1)$ is favored (see Sec. II below), and the corresponding constraints on the model parameters (especially H_0) will be significantly changed. Actually, the effect of F on H_0 was also discussed in e.g. [38] and Sec. 4.4 of [39], and it was found that a small F is required to obtain a Hubble constant H_0 consistent with the ones of Planck 2018 and SH0ES. Noting that $\sigma_\Delta = Fz^{-0.5}$ is related to the variance of the distribution of $\rm DM_{IGM}$, one of the possible ways out is to modify σ_Δ as in e.g. [37].

In the present work, at first we follow the Macquart's methodology in Sec. II, and an unusually low Hubble constant H_0 is found by using 125 localized FRBs if a loose prior $[\,0.01,\, 10.0\,]$ for the parameter F is allowed. Clearly, it is in great tension with the ones of Planck 2018 and SH0ES. On the other hand, we also consider the same priors used by Macquart *et al.* [32] (especially the same narrow prior $[\,0.011,\, 0.5\,]$ for F), and a higher H_0 could be found by requiring a small F in this case. But we show that the model with loose F prior is strongly preferred over the one with narrow F prior in all terms of the Bayesian evidence and the information criteria AIC, BIC. So, the great Hubble tension between FRBs, Planck 2018 and SH0ES should be taken seriously. Instead of modifying $\sigma_\Delta = Fz^{-0.5}$ in the distribution of $\rm DM_{IGM}$, here we try to find a new way out by generalizing the distribution of $\rm DM_{host}$. In Secs. III and IV, we consider the generalized distributions of $\rm DM_{host}$ with varying location and scale parameters ℓ and e^μ, respectively. We find that H_0 can be consistent with the ones of Planck 2018 and SH0ES in all cases. All the Bayesian evidence and the information criteria AIC, BIC for the generalized distributions of $\rm DM_{host}$ are overwhelmingly strong. Finally, some brief concluding remarks are given in Sec. V.

II. THE FIDUCIAL METHODOLOGY

A. The methodology and the data

At first, we follow the Macquart's methodology [32] to constrain the Hubble constant H_0 by using the current localized FRBs. The starting point is Eq. (1). For a given FRB with known right ascension (R.A.) and declination (Dec.), its $\rm DM_{MW,\,ISM}$ and $\rm DM_{MW,\,halo}$ can be found by using NE2001 [40, 41] and YT2020 [42], respectively. One can do that with PyGEDM [43, 44] incorporating NE2001/YMW16 and YT2020. Note that in this way $\rm DM_{MW,\,halo}$ is not a constant, slightly different from [32]. It is convenient to introduce the extragalactic DM, namely

$$\rm DM_E \equiv DM_{obs} - DM_{MW,\,ISM} - DM_{MW,\,halo} = DM_{IGM} + DM_{host}/(1+z)\,, \tag{3}$$

where we used Eq. (1) in the second step. The mean of $\rm DM_{IGM}$ at redshift z in Eq. (2) can be recast as

$$\langle {\rm DM_{IGM}}\rangle = \frac{3cf_e\cdot\Theta}{8\pi G m_p}\int_0^z \frac{(1+\tilde{z})\,d\tilde{z}}{E(\tilde{z})}\,, \qquad \Theta \equiv \Omega_b H_0 f_{\rm IGM} = \frac{\Omega_b h^2 f_{\rm IGM}}{H_0}\cdot (100~{\rm km/s/Mpc})^2\,, \tag{4}$$

where $f_e = 7/8$ as in e.g. [14–23], $h = H_0/(100~{\rm km/s/Mpc})$, Θ is in units of km/s/Mpc, and

$$E(z) \equiv H(z)/H_0 = \sqrt{\Omega_m\,(1+z)^3 + (1-\Omega_m)}\,, \tag{5}$$

for a flat ΛCDM cosmology in the Friedmann-Robertson-Walker (FRW) universe. In this work, we adopt $\Omega_m = 0.3153$ from the Planck 2018 result [4]. The combination Θ characterizes the degeneration between H_0, $\Omega_b h^2$ and $f_{\rm IGM}$. We regard Θ as a free model parameter, and H_0 can be derived from Θ if $\Omega_b h^2$ and $f_{\rm IGM}$ are given. As mentioned above, $\rm DM_{IGM}$ fluctuates around $\langle \rm DM_{IGM}\rangle$ due to the plasma density fluctuation along the line of sight. The distribution of $\rm DM_{IGM}$ is described by the following PDF [32]

FRB	R.A.	Dec.	$\mathrm{DM_{obs}}$	Redshift	Ref.	FRB	R.A.	Dec.	$\mathrm{DM_{obs}}$	Redshift	Ref.
20220207C	310.1995	72.8823	262.38	0.04304	[56, 57]	20220307B	350.8745	72.1924	499.27	0.248123	[56, 57]
20220310F	134.7204	73.4908	462.24	0.477958	[56, 57]	20220319D	32.1779	71.0353	110.98	0.011228	[56, 57]
20220418A	219.1056	70.0959	623.25	0.622	[56, 57]	20220506D	318.0448	72.8273	396.97	0.30039	[56, 57]
20220509G	282.67	70.2438	269.53	0.0894	[56, 57]	20220825A	311.9815	72.5850	651.24	0.241397	[56, 57]
20220914A	282.0568	73.3369	631.28	0.1139	[56, 57]	20220920A	240.2571	70.9188	314.99	0.158239	[56, 57]
20221012A	280.7987	70.5242	441.08	0.284669	[56, 57]	20220912A	347.2704	48.7071	219.46	0.0771	[58, 59]
20210117A	339.9792	−16.1515	729.1	0.214	[60]	20181220A	348.6982	48.3421	208.66	0.02746	[61, 62]
20181223C	180.9207	27.5476	111.61	0.03024	[61, 62]	20190418A	65.8123	16.0738	182.78	0.07132	[61, 62]
20190425A	255.6625	21.5767	127.78	0.03122	[61, 62]	20220610A	351.0732	−33.5137	1458.15	1.016	[63]
20200120E	149.4863	68.8256	87.782	−0.0001	[64]	20171020A	333.75	−19.6667	114.1	0.008672	[65]
20121102A	82.9946	33.1479	557.0	0.1927	[66]	20180301A	93.2268	4.6711	536.0	0.3304	[66, 67]
20180916B	29.5031	65.7168	347.8	0.0337	[62, 66]	20180924B	326.1053	−40.9000	362.42	0.3212	[66]
20181112A	327.3485	−52.9709	589.27	0.4755	[66]	20190102C	322.4157	−79.4757	363.6	0.2912	[66]
20190608B	334.0199	−7.8982	338.7	0.1178	[66, 68]	20190611B	320.7456	−79.3976	321.4	0.3778	[66]
20190711A	329.4192	−80.358	593.1	0.522	[32, 66]	20190714A	183.9797	−13.021	504.13	0.2365	[66, 68–70]
20191001A	323.3513	−54.7478	506.92	0.234	[66, 71]	20200430A	229.7064	12.3767	380.1	0.1608	[66, 68]
20200906A	53.4962	−14.0832	577.8	0.3688	[66, 68]	20201124A	77.0146	26.0607	415.3	0.0979	[66, 72]
20210320C	204.4608	−16.1227	384.8	0.2797	[66]	20210410D	326.0863	−79.3182	571.2	0.1415	[66, 73]
20210807D	299.2214	−0.7624	251.9	0.1293	[66]	20211127I	199.8082	−18.8378	234.83	0.0469	[66]
20211203C	204.5625	−31.3801	636.2	0.3439	[66]	20211212A	157.3509	1.3609	206.0	0.0707	[66]
20220105A	208.8039	22.4665	583.0	0.2785	[66]	20191106C	199.5801	42.9997	332.2	0.10775	[62, 74]
20200223B	8.2695	28.8313	201.8	0.06024	[62, 74]	20190110C	249.3185	41.4434	221.6	0.12244	[62, 74]
20190303A	207.9958	48.1211	223.2	0.064	[62, 75]	20180814A	65.6833	73.6644	190.9	0.068	[62, 75]
20210405I	255.3397	−49.5451	565.17	0.066	[76]	20191228A	344.4304	−28.5941	297.5	0.2432	[77]
20181030A	158.5838	73.7514	103.5	0.00385	[62, 78]	20190523A	207.065	72.4697	760.8	0.66	[79]
20190614D	65.0755	73.7067	959.2	0.6	[68, 80]	20210603A	10.2741	21.2263	500.147	0.1772	[81]
20231120A	143.9840	73.2847	437.737	0.0368	[57]	20230124A	231.9162	70.9681	590.574	0.0939	[57]
20230628A	166.7867	72.2818	344.952	0.127	[57]	20221101B	342.2162	70.6812	491.554	0.2395	[57]
20221113A	71.411	70.3074	411.027	0.2505	[57]	20231123B	242.5382	70.7851	396.857	0.2621	[57]
20230307A	177.7813	71.6956	608.854	0.2706	[57]	20221116A	21.2102	72.6539	643.448	0.2764	[57]
20230501A	340.0272	70.9222	532.471	0.3015	[57]	20230626A	235.6296	71.1335	452.723	0.327	[57]
20220208A	322.5751	70.0410	440.73	0.351	[57]	20220726A	73.9457	69.9291	686.232	0.3619	[57]
20220330D	163.7512	70.3508	467.788	0.3714	[57]	20220204A	274.2262	69.7225	612.584	0.4012	[57]
20230712A	167.3585	72.5578	587.567	0.4525	[57]	20230216A	156.4722	3.4368	828.289	0.531	[57]
20221027A	130.8718	72.1010	452.723	0.5422	[57]	20221219A	257.6298	71.6268	706.708	0.553	[57]
20221029A	141.9634	72.4523	1391.746	0.975	[57]	20240114A	321.9161	4.3292	527.65	0.13	[82]
20220501C	352.3792	−32.4907	449.5	0.381	[83]	20220725A	353.3152	−35.9903	290.4	0.1926	[83]
20220918A	17.5921	−70.8114	656.8	0.491	[83]	20221106A	56.7048	−25.5698	343.8	0.2044	[83]
20230526A	22.2326	−52.7173	361.4	0.157	[83]	20230708A	303.1155	−55.3563	411.51	0.105	[83]
20230902A	52.1398	−47.3335	440.1	0.3619	[83]	20231226A	155.3638	6.1102	329.9	0.1569	[83]
20240201A	149.9056	14.0880	374.5	0.042729	[83]	20240208A	159.2296	−0.9544	260.2	0.39	[83]
20240210A	8.7796	−28.2707	283.73	0.023686	[83]	20240310A	17.6219	−44.4394	601.8	0.127	[83]
20240318A	150.3932	37.6164	256.4	0.12	[83]	20230718A	128.1619	−40.4519	477.0	0.035	[83–85]
20201123A	263.67	−50.76	433.55	0.0507	[86, 87]	20230521B	351.036	71.1380	1342.9	1.354	[54]
20230814B	335.9747	73.0259	696.4	0.553	[54]	20231220A	123.9087	73.6599	491.2	0.3355	[54]
20240119A	224.4672	71.6118	483.1	0.376	[54]	20240123A	68.2625	71.9453	1462.0	0.968	[54]
20240213A	166.1683	74.0754	357.4	0.1185	[54]	20240215A	268.4413	70.2324	549.5	0.21	[54]
20240229A	169.9835	70.6762	491.15	0.287	[54]	20230203A	151.6616	35.6941	420.1	0.1464	[88]
20230222A	106.9604	11.2245	706.1	0.1223	[88]	20230222B	238.7391	30.8987	187.8	0.11	[88]
20230311A	91.1097	55.9460	364.3	0.1918	[88]	20230703A	184.6244	48.7299	291.3	0.1184	[88]
20230730A	54.6646	33.1593	312.5	0.2115	[88]	20230926A	269.1249	41.8143	222.8	0.0553	[88]
20231005A	246.028	35.4487	189.4	0.0713	[88]	20231011A	18.2411	41.7491	186.3	0.0783	[88]
20231017A	346.7543	36.6527	344.2	0.245	[88]	20231025B	270.7881	63.9891	368.7	0.3238	[88]
20231123A	82.6232	4.4755	302.1	0.0729	[88]	20231128A	199.5782	42.9927	331.6	0.1079	[88]
20231201A	54.5893	26.8177	169.4	0.1119	[88]	20231204A	207.9990	48.116	221.0	0.0644	[88]
20231206A	112.4428	56.2563	457.7	0.0659	[88]	20231223C	259.5446	29.4979	165.8	0.1059	[88]
20231229A	26.4678	35.1129	198.5	0.019	[88]	20231230A	72.7976	2.3940	131.4	0.0298	[88]
20220717A	293.3042	−19.2877	637.34	0.36295	[89]	20220529A	19.1042	20.6325	246.3	0.1839	[89, 90]
20240124A	321.9162	4.3501	526.9	0.269	[91]	20220222C	203.9045	−28.0269	1071.2	0.853	[92]
20220224C	166.6775	−22.9399	1140.2	0.6271	[92]	20230125D	150.2050	−31.5447	640.08	0.3265	[92]
20230503E	238.4300	−83.7753	483.74	0.32	[92]	20230613A	356.8527	−27.0528	483.51	0.3923	[92]
20230907D	187.1425	8.6581	1030.79	0.4638	[92]	20231010A	14.7320	−70.5964	442.59	0.61	[92]
20231020B	57.2782	−37.7699	952.2	0.4775	[92]	20231210F	50.4053	−35.7614	720.6	0.5	[92]
20190520B	240.5178	−11.2881	1201.0	0.2414	[66]	20220831A	338.6955	70.5384	1146.25	0.262	[54]
20240304B	182.997	11.813	2458.2	2.148	[93]	20250316A	182.4347	58.8491	161.82	0.0067	[94]
20241228A	216.3857	12.0250	246.3	0.1614	[95]						

TABLE I: The sample of current 131 localized FRBs. R.A./Dec. and $\mathrm{DM_{obs}}$ are in units of degree and $\mathrm{pc\,cm^{-3}}$, respectively. See the text for details.

$\lvert\,\Delta\text{AIC}\,\rvert$			
Level of empirical support for the model with the smaller AIC			
$0-2$	$4-7$	>10	
Weak	Mild	Strong	

$\lvert\,\Delta\text{BIC}\,\rvert$			
Evidence against the model with the larger BIC			
$0-2$	$2-6$	$6-10$	>10
Weak	Positive	Strong	Very strong

$\lvert\,\ln\mathcal{B}\,\rvert$			
Evidence against the model with the smaller $\mathcal{Z}$			
$0-1$	$1-2.5$	$2.5-5$	>5
Inconclusive	Weak	Moderate	Strong

TABLE II: The empirical strength of ΔAIC, ΔBIC [96] and $\ln\mathcal{B}$ [97, 98] (see also e.g. [99]).

$$P_{\rm IGM}(\Delta)=A\Delta^{-\beta}\exp\left[-\frac{\left(\Delta^{-\alpha}-C_0\right)^2}{2\alpha^2\sigma_\Delta^2}\right]\qquad \text{for}\quad \Delta>0\,, \tag{6}$$

and $P_{\rm IGM}(\Delta)=0$ for $\Delta\leq 0$, where $\Delta\equiv {\rm DM_{IGM}}/\langle{\rm DM_{IGM}}\rangle$, and $\alpha=\beta=3$ as in [32]. Following [32], one can adopt the parameterization

$$\sigma_\Delta=Fz^{-0.5}\,. \tag{7}$$

C_0 is determined by requiring $\langle\Delta\rangle=1$, and we can find A with the normalization of $P_{\rm IGM}$. On the other hand, the rest frame ${\rm DM_{host}}$ (in units of ${\rm pc\,cm^{-3}}$) is described by a log-normal distribution [32]

$$P_{\rm host}({\rm DM_{host}}\,|\,\mu,\,\sigma_{\rm host})=\frac{1}{\sigma_{\rm host}{\rm DM_{host}}\sqrt{2\pi}}\cdot\exp\left[-\frac{\left(\log{\rm DM_{host}}-\mu\right)^2}{2\sigma_{\rm host}^2}\right]\qquad \text{for}\quad {\rm DM_{host}}>0\,, \tag{8}$$

and $P_{\rm host}({\rm DM_{host}})=0$ for ${\rm DM_{host}}\leq 0$, where "log" gives the natural logarithm (we also use "ln" in this work alternatively). This distribution has a median value of e^μ (in units of ${\rm pc\,cm^{-3}}$) [32, 45]. Noting Eq. (3), for a given i-th FRB with known redshift z_i and model parameters, we have [32, 35, 37]

$$P_i({\rm DM}_{{\rm E},\,i}\,|\,z_i)=\int_0^{(1+z_i)\,{\rm DM}_{{\rm E},\,i}}P_{\rm host}({\rm DM_{host}}\,|\,\mu,\,\sigma_{\rm host})\,P_{\rm IGM}({\rm DM}_{{\rm E},\,i}-{\rm DM_{host}}/(1+z_i))\,d{\rm DM_{host}}\,, \tag{9}$$

where we have used $0\leq{\rm DM_{host}}=(1+z)({\rm DM_E}-{\rm DM_{IGM}})\leq(1+z)\,{\rm DM_E}$ from Eq. (3), and ${\rm DM}_{{\rm E},\,i}={\rm DM}_{{\rm obs},\,i}-{\rm DM}_{{\rm MW,\,ISM},\,i}-{\rm DM}_{{\rm MW,\,halo},\,i}$. Notice that the factor $(1+z)$ has been dropped in [32], since they argued that its effect could be small for their sample of only 8 localized FRBs. However, in the accompanying code [46] at GitHub for [32], the factor $(1+z)$ has been correctly considered, but in an alternative way (redefining ${\rm DM}'_{\rm host}={\rm DM_{host}}/(1+z)$ and then recasting Eq. (9) in terms of ${\rm DM}'_{\rm host}$). Our Eq. (9) corresponds to e.g. Eq. (8) of [35]. As is well known, if $y=cx$ and c is a constant, $P(y)=(1/c)\,P(x)=(1/c)\,P(y/c)$. So, we can recast Eq. (9) as

$$P_i({\rm DM}_{{\rm E},\,i}\,|\,z_i)=\frac{1}{\langle{\rm DM_{IGM}}\rangle_i}\int_0^{(1+z_i)\,{\rm DM}_{{\rm E},\,i}}P_{\rm host}({\rm DM_{host}}\,|\,\mu,\,\sigma_{\rm host})\,P_{\rm IGM}\left(\frac{{\rm DM}_{{\rm E},\,i}-{\rm DM_{host}}/(1+z_i)}{\langle{\rm DM_{IGM}}\rangle_i}\right)d{\rm DM_{host}}\,, \tag{10}$$

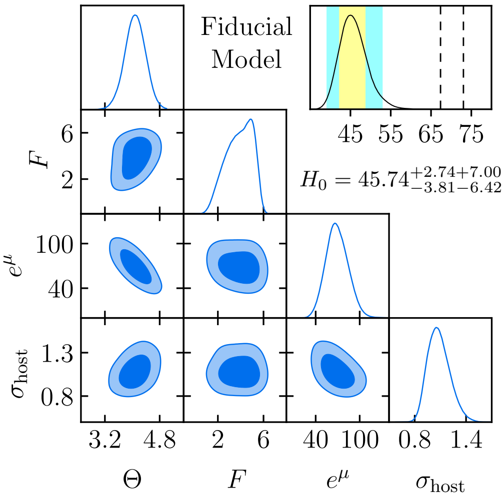

FIG. 1: The 1σ and 2σ contours for all the free parameters of the fiducial model. The top-right panel is the marginalized probability distribution of the Hubble constant H_0 derived from Θ in Eq. (4) by using $f_{\rm IGM} = 0.83$ and $\Omega_b h^2 = 0.02237$. The mean and 1σ, 2σ intervals of H_0 are given numerically and also shown by the shaded regions. Θ and H_0 are in units of km/s/Mpc. e^{μ} is in units of pc cm^{-3}. H_0 of the Planck 2018 and SH0ES results are also indicated by the vertical dashed lines. See Sec. II for details.

where $\langle {\rm DM_{IGM}} \rangle_i$ is $\langle {\rm DM_{IGM}} \rangle$ at redshift z_i. Our Eq. (10) corresponds to e.g. Eq. (20) or Eq. (A7) of [37] (equivalent to Eq. (A10) of [37] in terms of Δ). Notice that in the accompanying code [46] at GitHub for [32], the pre-factor $1/\langle {\rm DM_{IGM}} \rangle$ has been lost, and this point was independently found by e.g. [47, 48] and [37]. We refer to Appendix A of [37] for the detailed derivation. Finally, the total likelihood is given by the joint likelihoods of all localized FRBs [32], namely

$$\mathcal{L} = \prod_{i=1}^{N_{\rm FRB}} P_i({\rm DM}_{{\rm E},\,i} \,|\, z_i)\,. \tag{11}$$

We can maximize the likelihood $\mathcal{L}$ by using the Markov Chain Monte Carlo (MCMC) Python package Cobaya [49, 50] with GetDist [51, 52], and then obtain the constraints on the model parameters.

In Table I, we present the sample of current 131 localized FRBs. The redshift of FRB 20200120E is -0.0001, due to its peculiar velocity towards us, and hence it is decoupled from the cosmic expansion in fact. FRB 20190520B and 20220831A have extremely large ${\rm DM_{host}}$ [53, 54], while FRB 20190520B might be also influenced by the strong DM from intervening galaxies [55]. In addition, we also exclude FRB 20220319D, 20210405I, 20230718A, which are very close to us for their ${\rm DM_{obs}} < 1.5\ {\rm DM_{MW,\,ISM}}$. After these robust cuts, the remaining 125 localized FRBs will be used in this work.

B. The Bayesian evidence and the information criteria

For model comparison, the Bayesian evidence and the information criteria are needed. The Bayesian evidence is defined by [97, 98] (see also e.g. [99])

$$\mathcal{Z} = \int \mathcal{L}(\boldsymbol{\psi})\, \Phi(\boldsymbol{\psi})\, d\boldsymbol{\psi}\,, \tag{12}$$

where $\mathcal{L}$ is the likelihood function, Φ is the prior distribution, and $\boldsymbol{\psi}$ denotes the model parameters. For model comparison, it is convenient to use the Bayes factor

$$\mathcal{B}_{12} = \mathcal{Z}_1/\mathcal{Z}_2\,, \quad \text{or equivalently,} \quad \ln \mathcal{B}_{12} = \ln \mathcal{Z}_1 - \ln \mathcal{Z}_2\,, \tag{13}$$

where $\mathcal{Z}_1$ and $\mathcal{Z}_2$ are the Bayesian evidences for models Q_1 and Q_2, respectively. If $\mathcal{B}_{12}$ is larger (smaller) than 1, equivalently, if $\ln \mathcal{B}_{12}$ is positive (negative), model Q_1 (Q_2) is preferred over the other model. The

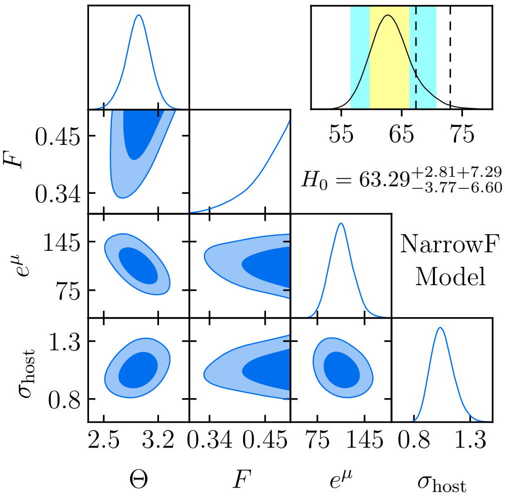

FIG. 2: The same as in Fig. 1, but for the narrow priors used by Macquart *et al.* [32]. See Sec. II for details.

strength of evidence is indicated by the empirical ranges of $|\ln\mathcal{B}\,|$ summarized in Table II [97, 98] (see also e.g. [99]). Note that one can compute the Bayesian evidence by using the nested sampling (such as PolyChord, dynesty, MultiNest, nessai), or alternatively MCEvidence with the MCMC chains [100–102]. On the other hand, some approximations of Bayesian evidence such as the Akaike information criterion (AIC) and the Bayesian information criterion (BIC) have been extensively used in the literature. The AIC is defined by [103]

$$\mathrm{AIC} = -2\ln\mathcal{L}_{\rm max} + 2\kappa\,, \tag{14}$$

where $\mathcal{L}_{\rm max}$ is the maximum likelihood, and κ is the number of free model parameters. In the Gaussian cases, $\chi^2_{\rm min} = -2\ln\mathcal{L}_{\rm max}$. The BIC is defined by [104]

$$\mathrm{BIC} = -2\ln\mathcal{L}_{\rm max} + \kappa\ln N\,, \tag{15}$$

where N is the number of data points. Comparing Eqs. (14) and (15), it is easy to see that BIC is much tougher than AIC for $\ln N > 2$. As is well known, a smaller AIC or BIC means a better fitting for the given model. We compare two models Q_1 and Q_2 by calculating the differences in AIC and BIC, namely $\Delta\mathrm{AIC}_{12} = \mathrm{AIC}_1 - \mathrm{AIC}_2$ and $\Delta\mathrm{BIC}_{12} = \mathrm{BIC}_1 - \mathrm{BIC}_2$. A negative (positive) $\Delta\mathrm{AIC}_{12}$ or $\Delta\mathrm{BIC}_{12}$ means a preference for model Q_1 (Q_2). The strength of evidence is indicated by the empirical ranges of $|\Delta\mathrm{AIC}\,|$ or $|\Delta\mathrm{BIC}\,|$ summarized in Table II [96] (see also e.g. [99]). In the followings, we will compare models with the Bayesian evidence and the information criteria AIC, BIC.

C. The fiducial model

Now, we can constrain the model parameters by using the methodology and current 125 localized FRBs given in Sec. II A. At first, we consider the fiducial model with the following uniform priors

$$\Theta \in [\,0.1,\, 5.0\,], \quad F \in [\,0.01,\, 10.0\,], \quad e^{\mu} \in [\,0.01,\, 400\,], \quad \sigma_{\rm host} \in [\,0.01,\, 4.0\,]\,. \tag{16}$$

This is the fiducial model, and the other models will be compared with it. Fitting to the data, we find the constraints on the free model parameters given by their means with 1σ uncertainties,

$$\Theta = 4.0818^{+0.3026}_{-0.2959}\,, \quad F = 3.8885^{+1.5362}_{-0.8217}\,, \quad e^{\mu} = 69.1945^{+14.1032}_{-15.9000}\,, \quad \sigma_{\rm host} = 1.0818^{+0.1004}_{-0.1525}\,. \tag{17}$$

We also present their contours in Fig. 1. As mentioned above, we adopt $\Omega_b h^2 = 0.02237$ from the Planck 2018 result [4] and $f_{\rm IGM} = 0.83$ [14–23] to derive the Hubble constant H_0 from Θ in Eq. (4), namely

$$H_0 = 45.7412^{+2.7429}_{-3.8149}\,(1\sigma)\ {}^{+6.9952}_{-6.4191}\,(2\sigma)\ {}^{+10.9120}_{-7.3231}\,(3\sigma)\ \mathrm{km/s/Mpc}\,. \tag{18}$$

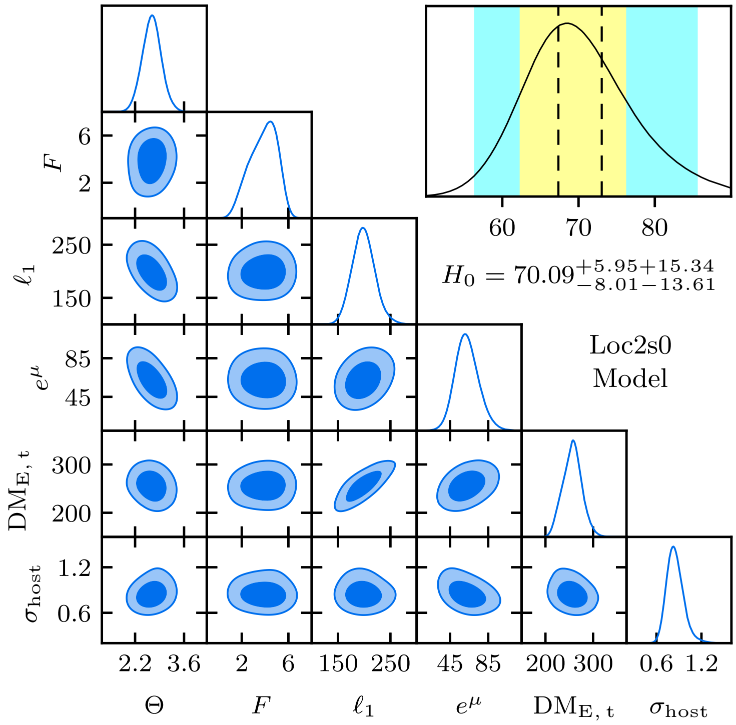

FIG. 3: The same as in Fig. 1, but for the Loc2s0 model. See Sec. III for details.

Notice that one can do this easily by defining derived parameters in the MCMC codes e.g. Cobaya or CosmoMC with GetDist. We also present the derived H_0 in the top-right panel of Fig. 1. It is easy to see that the Hubble constants of Planck 2018 and SH0ES (indicated by the vertical dashed lines in Fig. 1) is very far from the one of our fiducial model. So, a great tension exists (about $7 \sim 8\sigma$).

Note that we have adopted a loose prior $[\,0.01,\, 10.0\,]$ for the parameter F in the fiducial model, and all the model parameters (especially F) can be well constrained by the data in this case, as shown in Fig. 1. In the literature, the effect of F on H_0 was discussed in e.g. [38] and Sec. 4.4 of [39], and it was found that a small F is required to obtain a Hubble constant H_0 consistent with the ones of Planck 2018 and SH0ES. In fact, this is one of the keys in the Macquart's paper [32], which adopted a narrow prior for F with a fairly small upper bound 0.5. Here we also consider the same narrow priors as in Extended Data Table 2 of Macquart *et al.* [32], namely

$$\Theta \in [\,0.1,\, 5.0\,], \quad F \in [\,0.011,\, 0.5\,], \quad e^{\mu} \in [\,20,\, 200\,], \quad \sigma_{\mathrm{host}} \in [\,0.2,\, 2.0\,]\,. \tag{19}$$

They are all much narrower than the ones of our fiducial model in Eq. (16). We label it as the NarrowF model. Fitting to the data, we find the constraints on the free model parameters, namely

$$\Theta = 2.9426^{+0.1626}_{-0.1468}\,, \quad F = 0.4499^{+0.0501}_{-0.0112}\,, \quad e^{\mu} = 110.8110^{+14.8670}_{-19.0889}\,, \quad \sigma_{\mathrm{host}} = 1.0512^{+0.0831}_{-0.1152}\,, \tag{20}$$

and the derived Hubble constant

$$H_0 = 63.2876^{+2.8117}_{-3.7689}\,(1\sigma)\;{}^{+7.2854}_{-6.6005}\,(2\sigma)\;{}^{+10.9656}_{-7.8067}\,(3\sigma)\ \mathrm{km/s/Mpc}\,. \tag{21}$$

We also present the results in Fig. 2. In this small F case, H_0 can be consistent with the ones of Planck 2018 and SH0ES in 2σ and 3σ regions, respectively. However, we note that the marginalized probability distribution of F is skew, while F cannot be constrained from the right hand side, as shown in Fig. 2 (see also e.g. Fig. 5 of [37] and Extended Data Fig. 5 of [32]). The fairly small upper bound 0.5 of the narrow prior for F prevents it from taking larger values. If F can be larger (e.g. $F > 1 \sim 4$), H_0 will significantly become inconsistent with the ones of Planck 2018 and SH0ES, as shown by the fiducial model. In fact, $F \simeq 0.45$ of the NarrowF model is far outside 3σ region of the fiducial model (n.b. Eq. (17)).

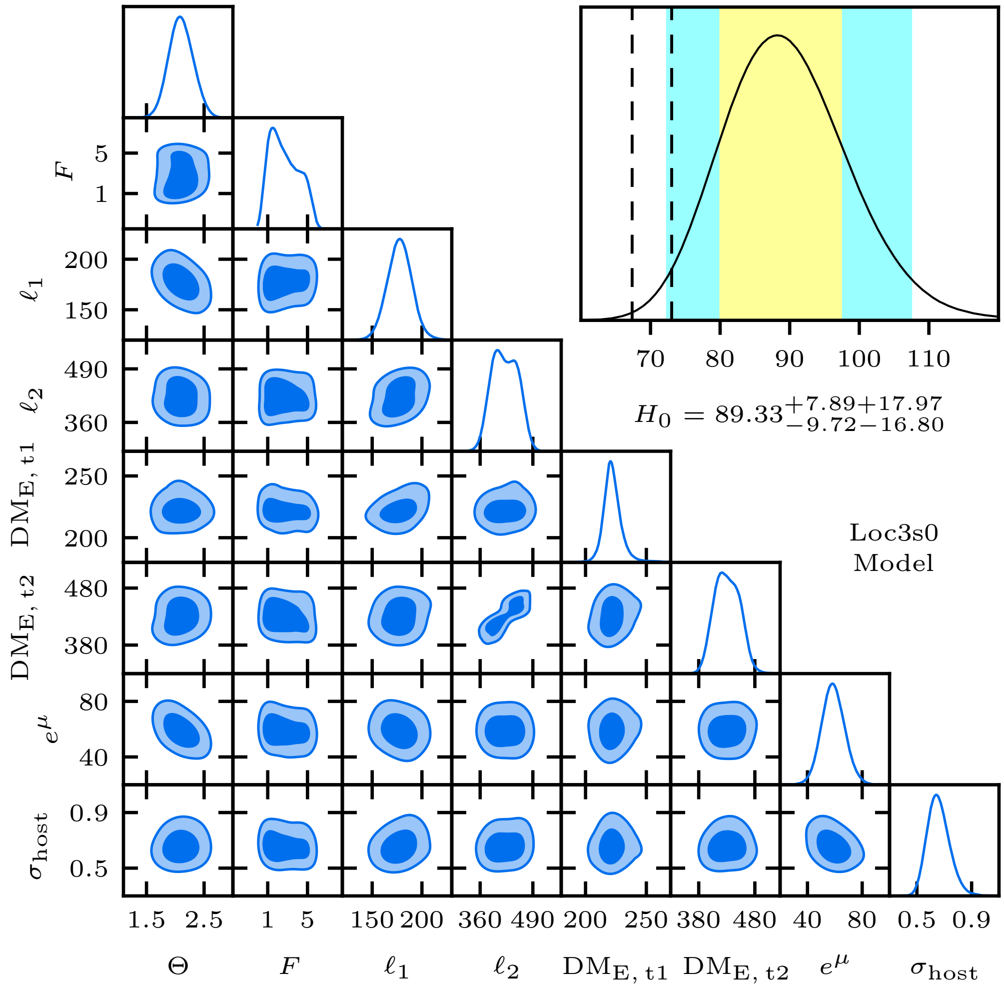

FIG. 4: The same as in Fig. 1, but for the Loc3s0 model. See Sec. III for details.

It is natural to see which model is better. We compute $\ln\mathcal{B}$, ΔAIC and ΔBIC of the NarrowF model relative to the fiducial model, and find

$$\ln\mathcal{B} = -6.6841\,, \quad \Delta\mathrm{AIC} = 13.4264\,, \quad \Delta\mathrm{BIC} = 13.4264\,. \tag{22}$$

Thus, the fiducial model is strongly preferred over the NarrowF model in terms of the Bayesian evidence and the information criteria AIC, BIC (n.b. Table II). So, the great Hubble tension between FRBs, Planck 2018 and SH0ES should be taken seriously.

III. GENERALIZED DISTRIBUTIONS OF $\mathrm{DM_{host}}$ WITH VARYING LOCATION ℓ

Instead of modifying $\sigma_\Delta = Fz^{-0.5}$ in the distribution of $\mathrm{DM_{IGM}}$, we try to find a new way out by generalizing the distribution of $\mathrm{DM_{host}}$ in the present work. Note that the log-normal distribution Eq. (8) used in the fiducial methodology is not the general form. According to e.g. [45], one can shift and/or scale the standard log-normal distribution by using the location and scale parameters. The general log-normal distribution of $\mathrm{DM_{host}}$ is given by [45]

$$P_{\mathrm{host}}(\mathrm{DM_{host}}\,|\,\ell,\,\mu,\,\sigma_{\mathrm{host}}) = \frac{1}{\sigma_{\mathrm{host}}\,(\mathrm{DM_{host}}-\ell)\,\sqrt{2\pi}}\cdot\exp\left[-\frac{\left(\log\left(\mathrm{DM_{host}}-\ell\right)-\mu\right)^2}{2\sigma_{\mathrm{host}}^2}\right]\,, \tag{23}$$

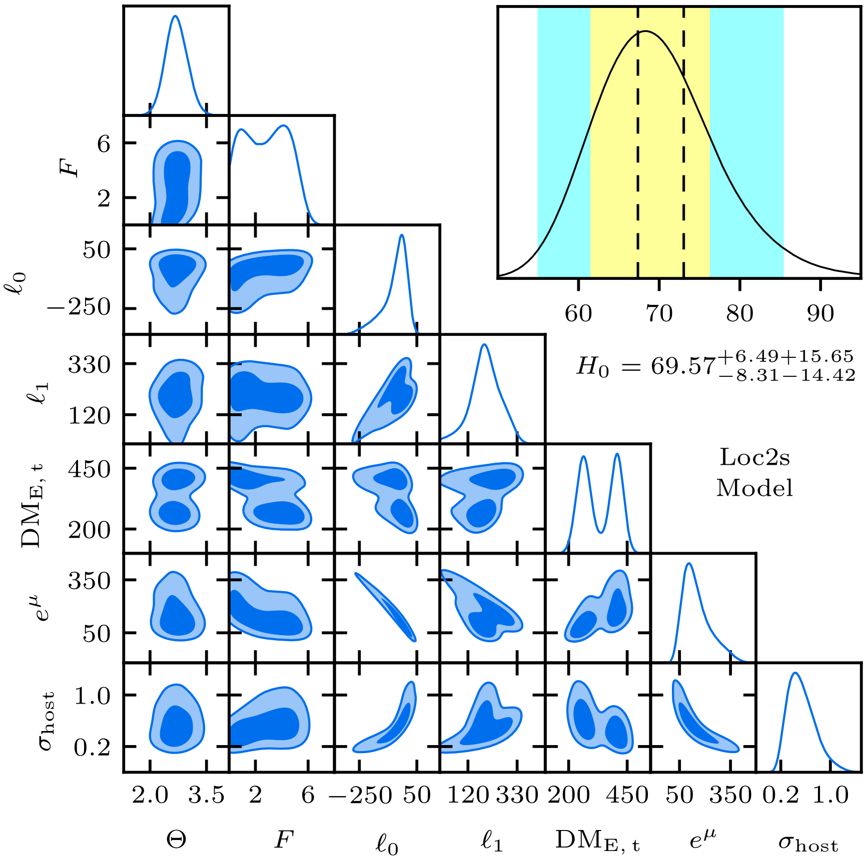

FIG. 5: The same as in Fig. 1, but for the Loc2s model. See Sec. III for details.

where ℓ and e^{μ} (both in uints of pc cm^{-3}) play the roles of location and scale parameters, respectively. In the fiducial methodology proposed by Macquart *et al.* [32], a zero location parameter $\ell = 0$ has been set. In fact, a non-zero location parameter ℓ shifts the log-normal distribution of $\mathrm{DM_{host}}$ as a whole. If $\ell > 0$, $\mathrm{DM_{host}}$ will be shifted toward larger values, or equivalently $\mathrm{DM_{IGM}}$ will be shifted toward smaller values for the fixed $\mathrm{DM_E} = \mathrm{DM_{IGM}} + \mathrm{DM_{host}}/(1+z)$, and hence Θ will be smaller (n.b. Eq. (4)). A smaller Θ leads to a larger Hubble constant H_0 for the fixed $\Omega_b h^2$ and $f_{\rm IGM}$. The physical picture is clear to make H_0 from localized FRBs consistent with the ones of Planck 2018 and SH0ES.

It is worth noting that one cannot make ℓ disappear by redefining $\mathrm{DM'_{host}} = \mathrm{DM_{host}} - \ell$ in $P_{\rm host}$. With this new $\mathrm{DM'_{host}}$, one should also change the integral variable $\mathrm{DM_{host}}$ in Eq. (9) to $\mathrm{DM'_{host}}$ accordingly, and then the term $\mathrm{DM_E} - \mathrm{DM_{host}}/(1+z)$ in $P_{\rm IGM}$ becomes $\mathrm{DM_E} - (\mathrm{DM'_{host}} + \ell)/(1+z)$. So, ℓ does not disappear but changes its position in the likelihood $\mathcal{L}$, and an $\ell > 0$ still leads to a larger H_0.

The naive idea to adopt a universal $\ell = const.$ does not work well. The key point is that $\mathrm{DM_{host}} - \ell > 0$ is required in Eq. (23). Thus, $\ell < \mathrm{DM_{host}} = (1+z)(\mathrm{DM_E} - \mathrm{DM_{IGM}}) \leq (1+z)\,\mathrm{DM_E}$. If $\ell = const.$ is universal for all localized FRBs, it should be less than the smallest $(1+z_i)\,\mathrm{DM_{E,\,\it i}}$ of all localized FRBs. This will force $\ell = const.$ to be fairly small (close to 0), not so different from the fiducial model.

By the way, we would like to talk about a minor technical detail. If $\ell \leq 0$, the lower limit of integral in Eq. (9) is still 0 since $\mathrm{DM_{host}} > 0$. But theoretically the lower limit of integral in Eq. (9) should be changed to ℓ if $\ell > 0$, due to the requirement $\mathrm{DM_{host}} > \ell$. In practice, however, we can still use a zero lower limit of integral in Eq. (9), because the integral from 0 to ℓ is zero actually, due to the fact that the log-normal PDF $f(x,\, s,\, loc,\, scale)$ in SciPy [45] returns 0 for $x \leq loc$. Even so, on the other hand, $\ell < (1+z)\,\mathrm{DM_E}$ is still required, otherwise the whole integral in Eq. (9) will be zero since $P_{\rm IGM}(\mathrm{DM_E} - \mathrm{DM_{host}}/(1+z)) = 0$ for $\mathrm{DM_{host}} > \ell \geq (1+z)\,\mathrm{DM_E}$ (n.b. $P_{\rm IGM}(\Delta) = 0$ for $\Delta \leq 0$ below Eq. (6)), and then the total likelihood $\mathcal{L} = 0$ or $\log\mathcal{L}$ diverges in the MCMC code. In summary, $\ell < \mathrm{DM_{host}} \leq (1+z)\,\mathrm{DM_E}$ is required, but technically the lower limit of integral in Eq. (9) can still be 0 in practice for convenience.

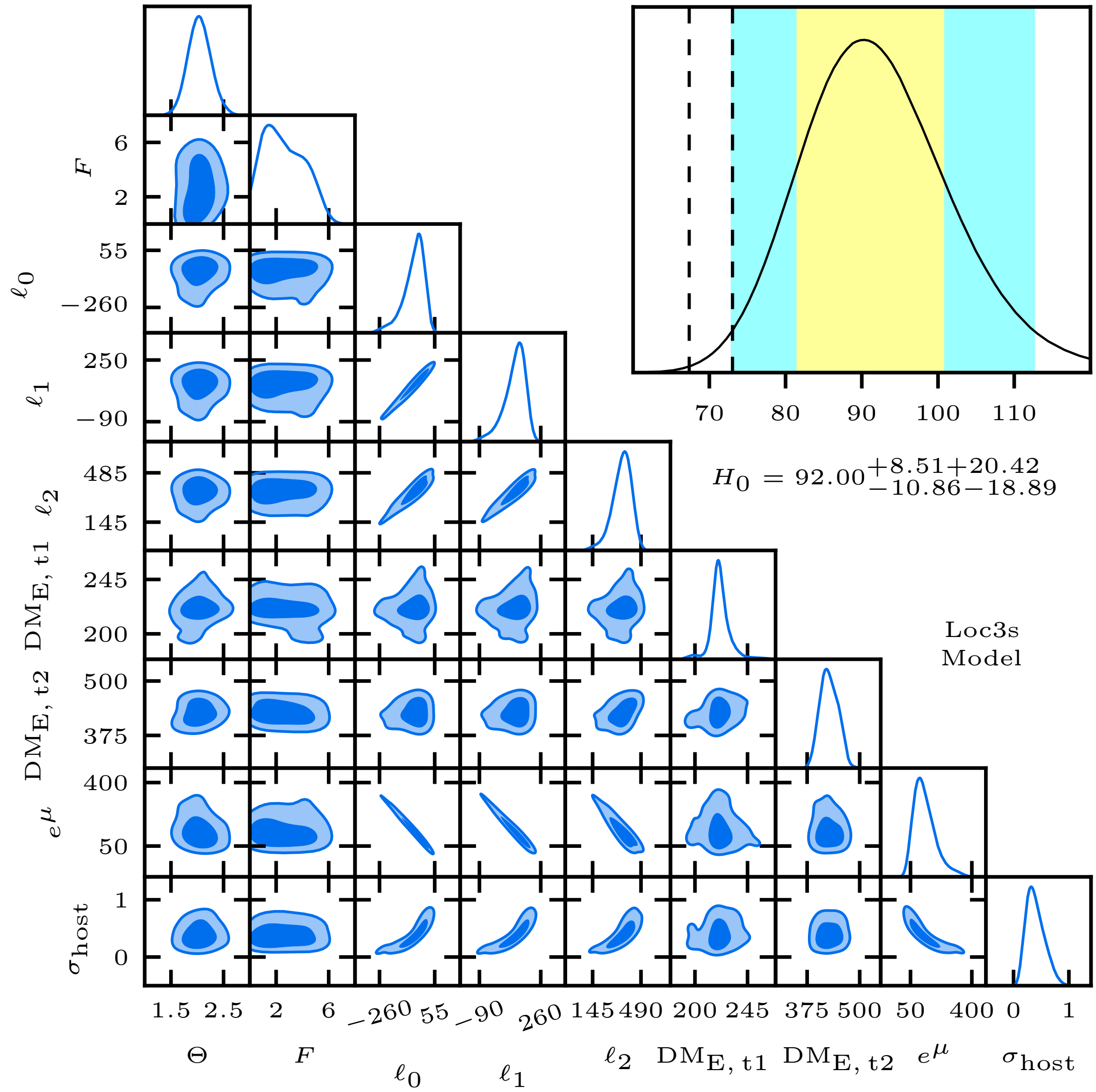

FIG. 6: The same as in Fig. 1, but for the Loc3s model. See Sec. III for details.

Let us come back. Since a universal $\ell = const.$ does not work well due to the FRBs with low values of $(1+z)\,\mathrm{DM_E}$ as mentioned above, it is reasonable to comfort these FRBs with a step-like ℓ, namely

$$\ell = \begin{cases} \ell_0 = 0 & \text{if } \ \mathrm{DM}_{\mathrm{E},\,i} < \mathrm{DM}_{\mathrm{E,\,t}}\,, \\ \ell_1 & \text{if } \ \mathrm{DM}_{\mathrm{E},\,i} \geq \mathrm{DM}_{\mathrm{E,\,t}}\,. \end{cases} \tag{24}$$

We label this model as Loc2s0, with two new model parameters ℓ_1 and $\mathrm{DM_{E,\,t}}$ (both in units of $\mathrm{pc\,cm^{-3}}$). It converges to the fiducial model for the FRBs with low $\mathrm{DM}_{\mathrm{E},\,i}$. Considering the following uniform priors

$$\Theta \in [\,0.01,\, 5.0\,]\,, \quad F \in [\,0.01,\, 10.0\,], \quad \ell_1 \in [\,0,\, 500\,]\,, \quad \mathrm{DM_{E,\,t}} \in [\,0.01,\, 1000\,]\,,$$
$$e^{\mu} \in [\,0.01,\, 400\,], \quad \sigma_{\rm host} \in [\,0.01,\, 4.0\,]\,, \tag{25}$$

and fitting to the data, we find the constraints on the free model parameters

$$\Theta = 2.6767^{+0.2593}_{-0.2700}\,, \quad F = 3.8628^{+1.4090}_{-0.9992}\,, \quad \ell_1 = 198.4876^{+20.4075}_{-21.3587}\,,$$
$$\mathrm{DM_{E,\,t}} = 256.1355^{+19.7559}_{-19.8058}\,, \quad e^{\mu} = 62.6493^{+10.9527}_{-13.1997}\,, \quad \sigma_{\rm host} = 0.8469^{+0.0912}_{-0.1226}\,. \tag{26}$$

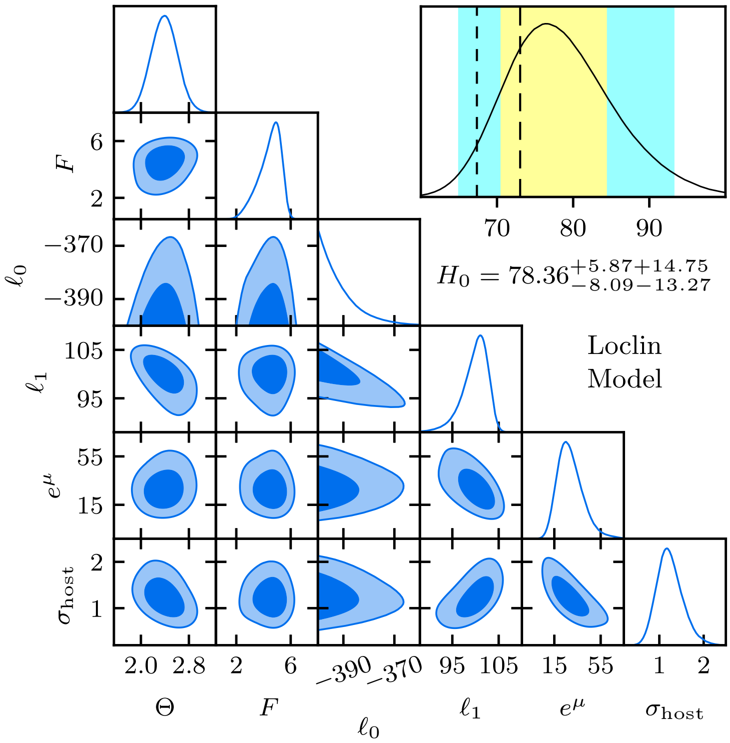

FIG. 7: The same as in Fig. 1, but for the Loclin model. See Sec. III for details.

As mentioned above, we adopt $\Omega_b h^2 = 0.02237$ from the Planck 2018 result [4] and $f_{\rm IGM} = 0.83$ [14–23] to derive the Hubble constant H_0 from Θ in Eq. (4), namely

$$H_0 = 70.0944^{+5.9540}_{-8.0131}\,(1\sigma)\;{}^{+15.3387}_{-13.6080}\,(2\sigma)\;{}^{+22.3251}_{-15.8234}\,(3\sigma)\;\,{\rm km/s/Mpc}\,. \tag{27}$$

We also present the results in Fig. 3. It is easy to see that H_0 is consistent with the ones of Planck 2018 and SH0ES well within 1σ region. We compute $\ln\mathcal{B}$, ΔAIC and ΔBIC of the Loc2s0 model relative to the fiducial model, and find

$$\ln\mathcal{B} = 37.2281\,,\quad \Delta{\rm AIC} = -86.2793\,,\quad \Delta{\rm BIC} = -80.6227\,. \tag{28}$$

Therefore, the Loc2s0 model is super-strongly preferred over the fiducial model in terms of the Bayesian evidence and the information criteria AIC, BIC (n.b. Table II). So, the generalized distributions of $\rm DM_{host}$ with ℓ works very well.

It is natural to go further by considering a three-step ℓ, namely

$$\ell = \begin{cases} \ell_0 = 0 & \text{if}\;\; {\rm DM}_{{\rm E},\,i} < {\rm DM}_{\rm E,\,t1}\,, \\ \ell_1 & \text{if}\;\; {\rm DM}_{\rm E,\,t1} \leq {\rm DM}_{{\rm E},\,i} < {\rm DM}_{\rm E,\,t2}\,, \\ \ell_2 & \text{if}\;\; {\rm DM}_{{\rm E},\,i} \geq {\rm DM}_{\rm E,\,t2}\,. \end{cases} \tag{29}$$

We label this model as Loc3s0, with four new model parameters ℓ_1, ℓ_2, ${\rm DM}_{\rm E,\,t1}$ and ${\rm DM}_{\rm E,\,t2}$ (all in units of ${\rm pc\,cm^{-3}}$). Notice that for convenience to give priors properly, we alternatively consider a free model parameter $S \geq 0$, and then regard ${\rm DM}_{\rm E,\,t2} = {\rm DM}_{\rm E,\,t1} + S$ as a derived parameter (the same below). This is just a technical trick to ensure ${\rm DM}_{\rm E,\,t2} \geq {\rm DM}_{\rm E,\,t1}$. Then, we consider the following uniform priors

$$\Theta \in [\,0.01,\,5.0\,]\,,\quad F \in [\,0.01,\,10.0\,],\quad \ell_1 \in [\,0,\,500\,]\,,\quad \ell_2 \in [\,0,\,1000\,]\,,$$
$${\rm DM}_{\rm E,\,t1} \in [\,0.01,\,500\,]\,,\quad S \in [\,0,\,500\,]\,,\quad e^{\mu} \in [\,0.01,\,400\,],\quad \sigma_{\rm host} \in [\,0.01,\,4.0\,]\,. \tag{30}$$

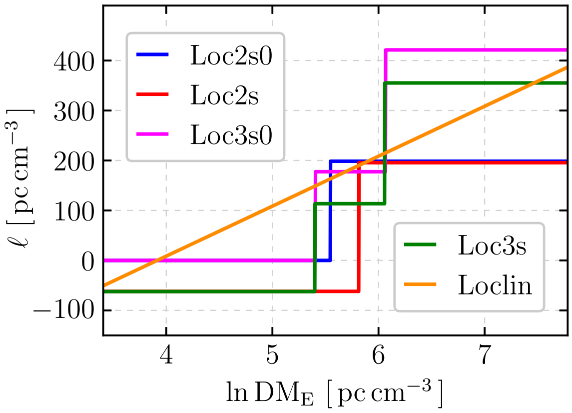

FIG. 8: ℓ versus $\ln \mathrm{DM_E}$ for all the ℓ models. See Sec. III for details.

Fitting to the data, we find the constraints on the free model parameters, namely

$$\Theta = 2.0991^{+0.1989}_{-0.2185}\,, \quad F = 2.7149^{+1.1196}_{-1.9822}\,, \quad \ell_1 = 177.4999^{+11.6885}_{-11.7157}\,, \quad \ell_2 = 421.2342^{+32.9453}_{-34.1844}\,,$$
$$\mathrm{DM_{E,\,t1}} = 222.2201^{+3.6458}_{-7.0353}\,, \quad S = 208.2475^{+21.7193}_{-23.3682}\,, \quad e^{\mu} = 58.7979^{+7.8195}_{-8.5305}\,,$$
$$\sigma_{\rm host} = 0.6563^{+0.0677}_{-0.0880}\,, \tag{31}$$

and the derived parameters

$$\mathrm{DM_{E,\,t2}} = 430.4676^{+22.6023}_{-23.2965}\,,$$
$$H_0 = 89.3252^{+7.8877}_{-9.7188}\,(1\sigma)\ {}^{+17.9703}_{-16.7970}\,(2\sigma)\ {}^{+25.5097}_{-20.9980}\,(3\sigma)\ \mathrm{km/s/Mpc}\,. \tag{32}$$

We also present the results in Fig. 4. This H_0 can be consistent with the ones of Planck 2018 and SH0ES in 3σ and 2σ regions, respectively. We compute $\ln \mathcal{B}$, ΔAIC and ΔBIC of the Loc3s0 model relative to the fiducial model, and find

$$\ln \mathcal{B} = 74.2829\,, \quad \Delta\mathrm{AIC} = -170.2343\,, \quad \Delta\mathrm{BIC} = -158.9210\,. \tag{33}$$

Therefore, the Loc3s0 model is ultra-strongly preferred over the fiducial model in terms of the Bayesian evidence and the information criteria AIC, BIC (n.b. Table II).

In the above cases, $\ell_0 = 0$ has been set. We can let it free, and consider

$$\ell = \begin{cases} \ell_0 & \text{if } \ \mathrm{DM}_{\mathrm{E},\,i} < \mathrm{DM_{E,\,t}}\,, \\ \ell_1 & \text{if } \ \mathrm{DM}_{\mathrm{E},\,i} \geq \mathrm{DM_{E,\,t}}\,. \end{cases} \tag{34}$$

We label this model as Loc2s. Fitting to the data with the following uniform priors

$$\Theta \in [\,0.01,\,5.0\,]\,, \quad F \in [\,0.01,\,10.0\,], \quad \ell_0 \in [\,-500,\,500\,]\,, \quad \ell_1 \in [\,0,\,500\,]\,,$$
$$\mathrm{DM_{E,\,t}} \in [\,0.01,\,1000\,]\,, \quad e^{\mu} \in [\,0.01,\,400\,], \quad \sigma_{\rm host} \in [\,0.01,\,4.0\,]\,, \tag{35}$$

we find the constraints on the free model parameters, namely

$$\Theta = 2.7004^{+0.2799}_{-0.3010}\,, \quad F = 2.9132^{+1.7648}_{-2.5270}\,, \quad \ell_0 = -61.9033^{+75.3180}_{-35.5040}\,, \quad \ell_1 = 195.6293^{+65.1040}_{-61.1179}\,,$$
$$\mathrm{DM_{E,\,t}} = 334.7655^{+78.7346}_{-80.8220}\,, \quad e^{\mu} = 149.0363^{+48.3310}_{-100.9250}\,, \quad \sigma_{\rm host} = 0.5313^{+0.1675}_{-0.2625}\,, \tag{36}$$

and the derived Hubble constant

$$H_0 = 69.5684^{+6.4939}_{-8.3134}\,(1\sigma)\ {}^{+15.6473}_{-14.4246}\,(2\sigma)\ {}^{+24.6636}_{-16.1807}\,(3\sigma)\ \mathrm{km/s/Mpc}\,. \tag{37}$$

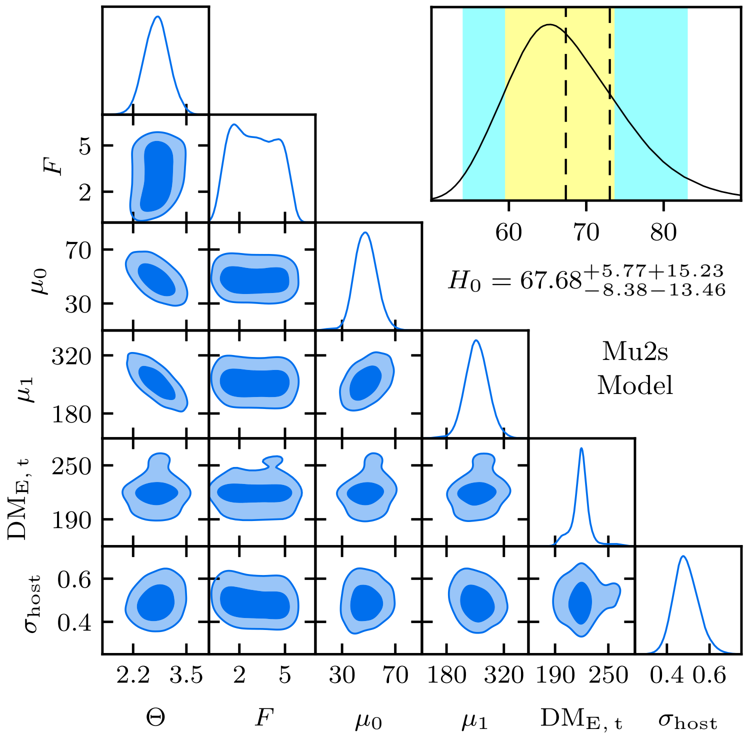

FIG. 9: The same as in Fig. 1, but for the Mu2s model. See Sec. IV for details.

We also present the results in Fig. 5. It is easy to see that H_0 is consistent with the ones of Planck 2018 and SH0ES well within 1σ region. We compute $\ln\mathcal{B}$, ΔAIC and ΔBIC of the Loc2s model relative to the fiducial model, and find

$$\ln\mathcal{B} = 34.4908\,, \quad \Delta\mathrm{AIC} = -84.0429\,, \quad \Delta\mathrm{BIC} = -75.5580\,. \tag{38}$$

Therefore, the Loc2s model is also super-strongly preferred over the fiducial model in terms of the Bayesian evidence and the information criteria AIC, BIC (n.b. Table II). It is of interest to compare the Loc2s model with the Loc2s0 model. Comparing Eqs. (28) and (38), one can see that the Loc2s0 model is mildly preferred over the Loc2s model, which has one more free parameter ℓ_0 but its reward is not good enough. On the other hand, $\ell_0 = 0$ is still in the 1σ region of ℓ_0 in Eq. (36) for the Loc2s model, and hence one can also understand the reason to prefer the Loc2s0 model.

Similarly, we also consider the Loc3s model, in which

$$\ell = \begin{cases} \ell_0 & \text{if } \mathrm{DM}_{\mathrm{E},\,i} < \mathrm{DM}_{\mathrm{E,\,t1}}\,, \\ \ell_1 & \text{if } \mathrm{DM}_{\mathrm{E,\,t1}} \leq \mathrm{DM}_{\mathrm{E},\,i} < \mathrm{DM}_{\mathrm{E,\,t2}}\,, \\ \ell_2 & \text{if } \mathrm{DM}_{\mathrm{E},\,i} \geq \mathrm{DM}_{\mathrm{E,\,t2}}\,, \end{cases} \tag{39}$$

and $\mathrm{DM}_{\mathrm{E,\,t2}} = \mathrm{DM}_{\mathrm{E,\,t1}} + S$ is a derived parameter, while $S \geq 0$ is a free model parameter, as mentioned above. We consider the Loc3s model with the following uniform priors

$$\Theta \in [\,0.01,\, 5.0\,]\,, \quad F \in [\,0.01,\, 10.0\,]\,, \quad \ell_0 \in [\,-300,\, 300\,]\,, \quad \ell_1 \in [\,-300,\, 1000\,]\,, \quad \ell_2 \in [\,0,\, 1000\,]\,,$$
$$\mathrm{DM}_{\mathrm{E,\,t1}} \in [\,0.01,\, 500\,]\,, \quad S \in [\,0.01,\, 500\,]\,, \quad e^{\mu} \in [\,0.01,\, 400\,]\,, \quad \sigma_{\rm host} \in [\,0.01,\, 4.0\,]\,. \tag{40}$$

Fitting to the data, we find the constraints on the free model parameters, namely

$$\Theta = 2.0415^{+0.2086}_{-0.2244}\,, \quad F = 2.6771^{+1.1196}_{-2.1358}\,, \quad \ell_0 = -62.2804^{+67.4354}_{-36.9136}\,, \quad \ell_1 = 113.5080^{+70.5603}_{-39.9469}\,,$$
$$\ell_2 = 355.0868^{+77.1831}_{-53.3624}\,, \quad \mathrm{DM}_{\mathrm{E,\,t1}} = 221.2832^{+5.5862}_{-7.2066}\,, \quad S = 205.8632^{+21.1272}_{-22.7897}\,,$$
$$e^{\mu} = 129.6882^{+39.8932}_{-73.8232}\,, \quad \sigma_{\rm host} = 0.3914^{+0.1248}_{-0.2001}\,, \tag{41}$$

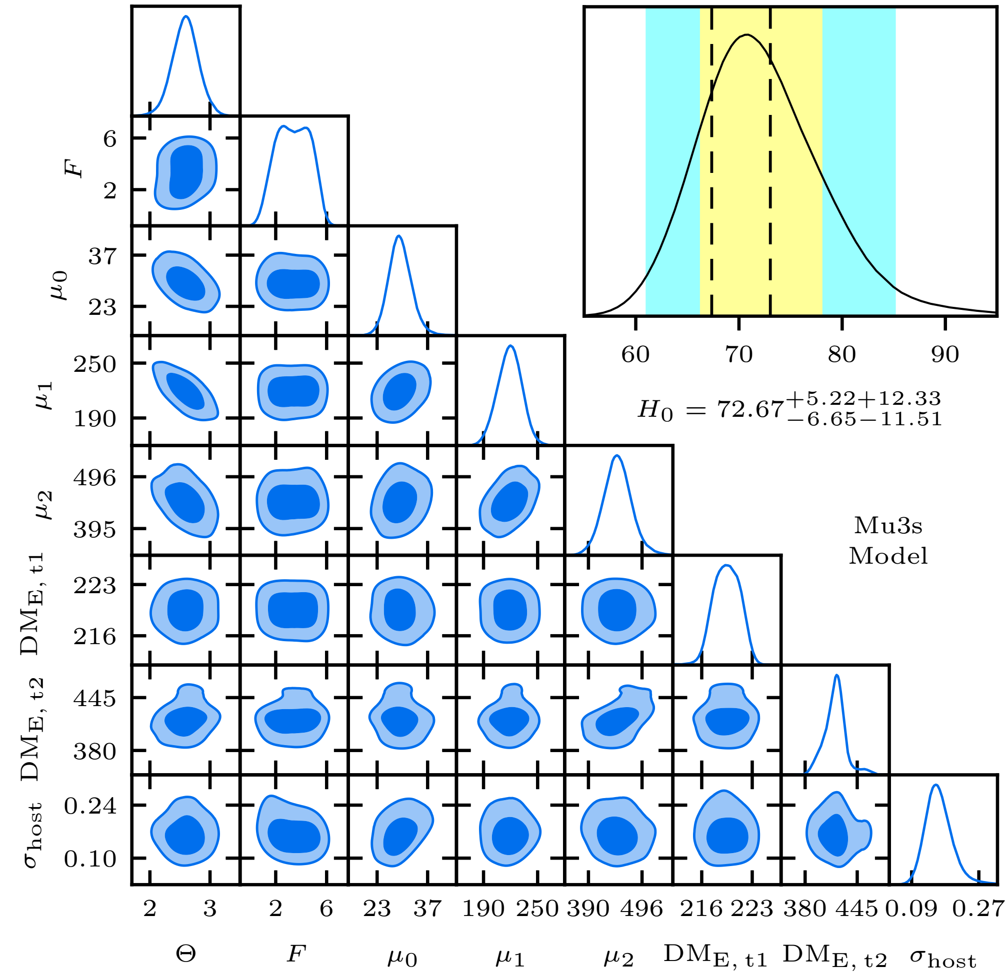

FIG. 10: The same as in Fig. 1, but for the Mu3s model. See Sec. IV for details.

and the derived parameters

$$\mathrm{DM_{E,\,t2}} = 427.1464^{+20.9173}_{-23.1121}\,,$$
$$H_0 = 91.9963^{+8.5124}_{-10.8584}\,(1\sigma)\ ^{+20.4240}_{-18.8946}\,(2\sigma)\ ^{+32.3452}_{-21.0885}\,(3\sigma)\ \mathrm{km/s/Mpc}\,. \tag{42}$$

We also present the results in Fig. 6. This H_0 can be consistent with the ones of Planck 2018 and SH0ES around 3σ and 2σ regions, respectively. We compute $\ln\mathcal{B}$, ΔAIC and ΔBIC of the Loc3s model relative to the fiducial model, and find

$$\ln\mathcal{B} = 71.7355\,, \quad \Delta\mathrm{AIC} = -168.8822\,, \quad \Delta\mathrm{BIC} = -154.7406\,. \tag{43}$$

Therefore, the Loc3s model is ultra-strongly preferred over the fiducial model in terms of the Bayesian evidence and the information criteria AIC, BIC (n.b. Table II). Comparing Eqs. (33) and (43), we find that the Loc3s0 model is mildly preferred over the Loc3s model, which has one more free parameter ℓ_0 but its reward is not good enough. This point is also supported by the fact that $\ell_0 = 0$ is still in the 1σ region of ℓ_0 in Eq. (41) for the Loc3s model.

All the above models are step-like. Could we find a suitable function for ℓ? In fact, we know ℓ poorly. Instead of guess, we might consider its Taylor expansion with respect to $\mathrm{DM_E}$ up to first order, namely $\ell = \ell_0 + \ell_1\mathrm{DM_E}$. However, $\mathrm{DM_E}$ of FRBs are large numbers spanning three magnitudes $\mathcal{O}(10 \sim 10^3)$. In this case, the higher orders cannot be dropped. Usually, one can smooth it by using logarithm. So, it is

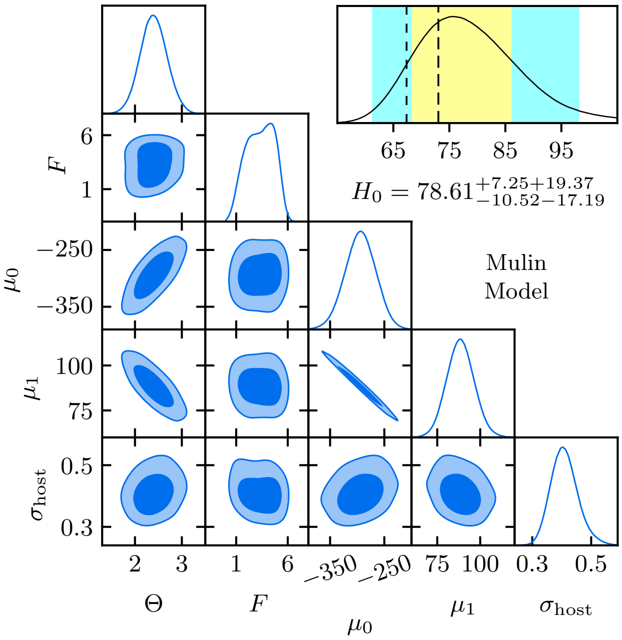

FIG. 11: The same as in Fig. 1, but for the Mulin model. See Sec. IV for details.

more reasonable to consider ℓ's Taylor expansion with respect to $\ln \mathrm{DM_E}$ up to first order, namely

$$\ell = \ell_0 + \ell_1 \ln \mathrm{DM_E}\,. \tag{44}$$

We label this model as Loclin. We consider the following uniform priors

$$\Theta \in [\,0.01,\, 5.0\,]\,, \quad F \in [\,0.01,\, 10.0\,], \quad \ell_0 \in [\,-400,\, 400\,]\,, \quad \ell_1 \in [\,0,\, 500\,]\,,$$
$$e^{\mu} \in [\,0.01,\, 400\,], \quad \sigma_{\rm host} \in [\,0.01,\, 4.0\,]\,. \tag{45}$$

Fitting to the data, we find the constraints on the free model parameters, namely

$$\Theta = 2.3897^{+0.2159}_{-0.2185}\,, \quad F = 4.4940^{+0.9577}_{-0.5750}\,, \quad \ell_0 = -391.1961^{+1.4323}_{-8.8039}\,, \quad \ell_1 = 99.9552^{+3.1191}_{-1.8468}\,,$$
$$e^{\mu} = 28.5563^{+8.1344}_{-12.3782}\,, \quad \sigma_{\rm host} = 1.2324^{+0.2391}_{-0.3209}\,, \tag{46}$$

and the derived Hubble constant

$$H_0 = 78.3573^{+5.8734}_{-8.0948}\,(1\sigma)\ {}^{+14.7481}_{-13.2660}\,(2\sigma)\ {}^{+21.8856}_{-15.8673}\,(3\sigma)\ \mathrm{km/s/Mpc}\,. \tag{47}$$

We also present the results in Fig. 7. One can see that H_0 can be consistent with the ones of Planck 2018 and SH0ES in 2σ and 1σ regions, respectively. We compute $\ln \mathcal{B}$, ΔAIC and ΔBIC of the Loclin model relative to the fiducial model, and find

$$\ln \mathcal{B} = 49.1156\,, \quad \Delta\mathrm{AIC} = -112.5922\,, \quad \Delta\mathrm{BIC} = -104.1073\,. \tag{48}$$

Therefore, the Loclin model is super-strongly preferred over the fiducial model in terms of the Bayesian evidence and the information criteria AIC, BIC (n.b. Table II).

It is of interest to compare all the ℓ models. In Fig. 8, we present ℓ versus $\ln \mathrm{DM_E}$ for all the ℓ models, while the model parameters take their mean values obtained from the data. We find that $\ell_0 \sim -60$ or 0, and $\ell_1 \sim 200$ or 100 for all step-like ℓ models, while the transition(s) might happen at $\ln \mathrm{DM_E} \sim 5.5$. The ℓ of Loclin model crosses almost all steps of ℓ_i, as shown in Fig. 8, and hence this linear ℓ model is at least a decent enough approximation of the unknown ℓ function. The common feature of all the ℓ models is that ℓ converges to a small value (around 0) to comfort the localized FRBs at low $\mathrm{DM_E}$ as in the

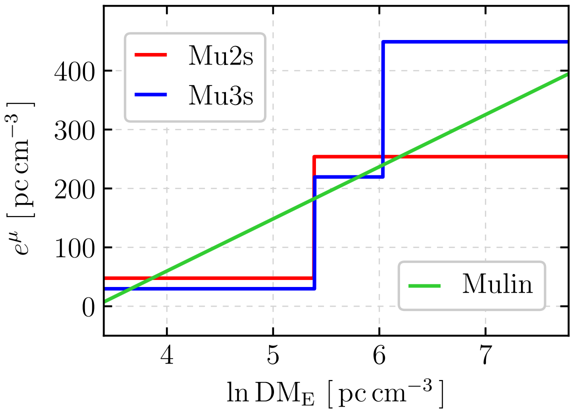

FIG. 12: e^{μ} versus $\ln \mathrm{DM_E}$ for all the e^{μ} models. See Sec. IV for details.

fiducial model, and then ℓ becomes larger at high $\mathrm{DM_E}$ to shift the Hubble constant H_0. The physical picture is quite clear. On the other hand, in Table III, we also summarize the Bayesian evidences and the information criteria AIC, BIC for all the ℓ models relative to the fiducial model. One can easily see that Loc3s0 $>$ Loc3s $\gg$ Loclin $\gg$ Loc2s0 $>$ Loc2s $\gg$ Fiducial. All the ℓ models are overwhelmingly preferred over the fiducial model in terms of the Bayesian evidence and the information criteria AIC, BIC. The Hubble constants H_0 can be consistent with the ones of Planck 2018 and SH0ES in all the ℓ models.

IV. GENERALIZED DISTRIBUTIONS OF $\mathrm{DM_{host}}$ WITH VARYING SCALE e^{μ}

As discussed in the beginning of Sec. III, the key to make the Hubble constant H_0 be consistent with the ones of Planck 2018 and SH0ES is to shift $\mathrm{DM_{host}}$ toward larger values. In Sec. III, we use the location parameter ℓ to this end, which shifts the log-normal distribution of $\mathrm{DM_{host}}$ as a whole. In this section, we try an alternative way. Let us come back to Eq. (8) without the location parameter ℓ (namely $\ell = 0$), and we note that the $\mathrm{DM_{host}}$ distribution in Eq. (8) has a median value of e^{μ} (in units of $\mathrm{pc\,cm^{-3}}$) [32, 45], which plays the role of scale parameter. If the median value e^{μ} of the log-normal $\mathrm{DM_{host}}$ distribution is shifted toward higher values, we can also get larger $\mathrm{DM_{host}}$ from this scaled log-normal distribution. The difference is that ℓ directly shifts the log-normal distribution as a whole, but e^{μ} only shifts the median value of the log-normal distribution, and hence it works indirectly. Even though, the scale parameter e^{μ} can also make H_0 consistent with the ones of Planck 2018 and SH0ES, but its indirect effects might be slightly weaker than ℓ. The physical picture is also clear.

Similar to the case of ℓ, one cannot make e^{μ} disappear by redefining $\mathrm{DM'_{host}} = \mathrm{DM_{host}}/e^{\mu}$ in $P_{\rm host}$. With this new $\mathrm{DM'_{host}}$, one should also change the integral variable $\mathrm{DM_{host}}$ in Eq. (9) to $\mathrm{DM'_{host}}$ accordingly, and then the term $\mathrm{DM_E} - \mathrm{DM_{host}}/(1+z)$ in $P_{\rm IGM}$ becomes $\mathrm{DM_E} - e^{\mu}\,\mathrm{DM'_{host}}/(1+z)$. So, e^{μ} does not disappear but changes its position in the likelihood $\mathcal{L}$, and a larger e^{μ} still leads to a higher H_0.

In the fiducial model, e^{μ} is a universal constant for all localized FRBs. But we want to shift e^{μ} toward larger values for the localized FRBs at high $\mathrm{DM_E}$, and also comfort the localized FRBs at low $\mathrm{DM_E}$ as in the fiducial model with smaller e^{μ}, similar to the cases of ℓ in Sec. III. Here, we still use the log-normal distribution of $\mathrm{DM_{host}}$ in Eq. (8) without the location parameter ℓ (namely $\ell = 0$), but we instead consider a step-like e^{μ} to this end, namely

$$e^{\mu} = \begin{cases} \mu_0 & \text{if} \;\; \mathrm{DM}_{\mathrm{E},\,i} < \mathrm{DM}_{\mathrm{E,\,t}}\,, \\ \mu_1 & \text{if} \;\; \mathrm{DM}_{\mathrm{E},\,i} \geq \mathrm{DM}_{\mathrm{E,\,t}}\,. \end{cases} \tag{49}$$

We label this model as Mu2s, with three new model parameters μ_0, μ_1, $\mathrm{DM_{E,\,t}}$ (all in units of $\mathrm{pc\,cm^{-3}}$). Fitting to the data with the following uniform priors

$$\Theta \in [\,0.01,\, 5.0\,]\,, \quad F \in [\,0.01,\, 10.0],\quad \mu_0 \in [\,0.01,\, 500\,]\,, \quad \mu_1 \in [\,0.01,\, 500\,]\,,$$
$$\mathrm{DM_{E,\,t}} \in [\,0.01,\, 1000\,]\,, \quad \sigma_{\rm host} \in [\,0.01,\, 4.0\,]\,, \tag{50}$$

Model	$\ln\mathcal{B}$	ΔAIC	ΔBIC	Model	$\ln\mathcal{B}$	ΔAIC	ΔBIC
Loc2s0	37.2281	−86.2793	−80.6227	Mu2s	29.3173	−70.9404	−65.2838
Loc3s0	74.2829	−170.2343	−158.9210	Mu3s	50.9335	−127.0943	−115.7810
Loc2s	34.4908	−84.0429	−75.5580	Mulin	39.1411	−90.0874	−87.2591
Loc3s	71.7355	−168.8822	−154.7406	Fiducial	0	0	0
Loclin	49.1156	−112.5922	−104.1073	NarrowF	−6.6841	13.4264	13.4264

TABLE III: The Bayesian evidences and the information criteria AIC, BIC for all models relative to the fiducial model (n.b. Table II).

we find the constraints on the free model parameters, namely

$$\Theta = 2.7765^{+0.2987}_{-0.3008}\,, \quad F = 3.0232^{+1.4360}_{-1.6360}\,, \quad \mu_0 = 47.6798^{+7.8199}_{-8.4040}\,, \quad \mu_1 = 253.9695^{+27.5511}_{-27.6963}\,,$$
$$\mathrm{DM_{E,\,t}} = 217.9626^{+10.3313}_{-9.2694}\,, \quad \sigma_{\rm host} = 0.4903^{+0.0512}_{-0.0628}\,, \tag{51}$$

and the derived Hubble constant

$$H_0 = 67.6841^{+5.7690}_{-8.3759}\,(1\sigma)\;{}^{+15.2261}_{-13.4556}\,(2\sigma)\;{}^{+24.8543}_{-15.2604}\,(3\sigma)\ \mathrm{km/s/Mpc}\,. \tag{52}$$

We also present the results in Fig. 9. It is easy to see that the Hubble constant H_0 can be consistent with the ones of Planck 2018 and SH0ES well within 1σ region. We compute $\ln\mathcal{B}$, ΔAIC and ΔBIC of the Mu2s model relative to the fiducial model, and find

$$\ln\mathcal{B} = 29.3173\,, \quad \Delta\mathrm{AIC} = -70.9404\,, \quad \Delta\mathrm{BIC} = -65.2838\,. \tag{53}$$

Therefore, the Mu2s model is super-strongly preferred over the fiducial model in terms of the Bayesian evidence and the information criteria AIC, BIC (n.b. Table II). So, the generalized distributions of $\mathrm{DM_{host}}$ with e^μ also works very well.

It is natural to go further with a three-step e^μ, namely

$$e^\mu = \begin{cases} \mu_0 & \text{if}\ \ \mathrm{DM}_{\mathrm{E},\,i} < \mathrm{DM_{E,\,t1}}\,, \\ \mu_1 & \text{if}\ \ \mathrm{DM_{E,\,t1}} \leq \mathrm{DM}_{\mathrm{E},\,i} < \mathrm{DM_{E,\,t2}}\,, \\ \mu_2 & \text{if}\ \ \mathrm{DM}_{\mathrm{E},\,i} \geq \mathrm{DM_{E,\,t2}}\,. \end{cases} \tag{54}$$

We label this model as Mu3s. Note that $\mathrm{DM_{E,\,t2}} = \mathrm{DM_{E,\,t1}} + S$ is a derived parameter, while $S \geq 0$ is a free model parameter, as mentioned above. Fitting to the data with the following uniform priors

$$\Theta \in [\,0.01,\,5.0\,]\,, \quad F \in [\,0.01,\,10.0],\quad \mu_0 \in [\,0.01,\,500\,]\,, \quad \mu_1 \in [\,0.01,\,500\,]\,,$$
$$\mu_2 \in [\,0.01,\,1000\,]\,, \quad \mathrm{DM_{E,\,t1}} \in [\,0.01,\,500\,]\,, \quad S \in [\,0.01,\,500\,]\,, \quad \sigma_{\rm host} \in [\,0.01,\,4.0\,]\,, \tag{55}$$

we find the constraints on the free model parameters, namely

$$\Theta = 2.5732^{+0.2140}_{-0.2152}\,, \quad F = 3.2902^{+1.5336}_{-1.4710}\,, \quad \mu_0 = 29.7024^{+2.5550}_{-3.7114}\,, \quad \mu_1 = 219.5306^{+12.5569}_{-12.5409}\,,$$
$$\mu_2 = 449.0181^{+25.4818}_{-26.5738}\,, \quad \mathrm{DM_{E,\,t1}} = 219.0075^{+2.6249}_{-1.8795}\,, \quad S = 198.1943^{+11.9329}_{-12.0856}\,,$$
$$\sigma_{\rm host} = 0.1659^{+0.0286}_{-0.0416}\,, \tag{56}$$

and the derived parameters

$$\mathrm{DM_{E,\,t2}} = 417.2018^{+11.8612}_{-11.2237}\,,$$
$$H_0 = 72.6672^{+5.2201}_{-6.6462}\,(1\sigma)\;{}^{+12.3322}_{-11.5107}\,(2\sigma)\;{}^{+18.4687}_{-13.6660}\,(3\sigma)\ \mathrm{km/s/Mpc}\,. \tag{57}$$

We also present the results in Fig. 10. It is easy to see that the Hubble constant H_0 can be consistent with the ones of Planck 2018 and SH0ES well within 1σ region. We compute $\ln\mathcal{B}$, ΔAIC and ΔBIC of the Mu3s model relative to the fiducial model, and find

$$\ln\mathcal{B} = 50.9335\,, \quad \Delta\text{AIC} = -127.0943\,, \quad \Delta\text{BIC} = -115.7810\,. \tag{58}$$

Therefore, the Mu3s model is ultra-strongly preferred over the fiducial model in terms of the Bayesian evidence and the information criteria AIC, BIC (n.b. Table II).

It is of interest to find a suitable e^{μ} function instead of step-like e^{μ}. Since we know e^{μ} poorly, a naive way is to consider its Taylor expansion with respect to $\ln \text{DM}_\text{E}$ up to first order, namely

$$e^{\mu} = \mu_0 + \mu_1 \ln \text{DM}_\text{E}\,. \tag{59}$$

We label this model as Mulin. Note that the Taylor expansion with respect to DM_E does not work, since DM_E of FRBs are large numbers spanning three magnitudes $\mathcal{O}(10 \sim 10^3)$ and hence the higher orders cannot be dropped, as discussed in Sec. III about the Loclin model. Fitting to the data with the following uniform priors

$$\begin{gathered}\Theta \in [\,0.01,\, 5.0\,]\,, \quad F \in [\,0.01,\, 10.0\,], \\ \mu_0 \in [\,-1000,\, 200\,]\,, \quad \mu_1 \in [\,-10,\, 500\,]\,, \quad \sigma_\text{host} \in [\,0.01,\, 4.0\,]\,, \end{gathered} \tag{60}$$

we find the constraints on the free model parameters, namely

$$\begin{gathered}\Theta = 2.3961^{+0.2836}_{-0.2820}\,, \quad F = 3.3718^{+1.5438}_{-1.3107}\,, \\ \mu_0 = -294.1853^{+28.4648}_{-27.8595}\,, \quad \mu_1 = 88.5052^{+8.0103}_{-7.9741}\,, \quad \sigma_\text{host} = 0.4092^{+0.0396}_{-0.0496}\,, \end{gathered} \tag{61}$$

and the derived Hubble constant

$$H_0 = 78.6095^{+7.2486}_{-10.5179}\,(1\sigma)\;^{+19.3653}_{-17.1903}\,(2\sigma)\;^{+31.3955}_{-19.1908}\,(3\sigma)\ \text{km/s/Mpc}\,. \tag{62}$$

We also present the results in Fig. 11. It is easy to see that the Hubble constant H_0 can be consistent with the ones of Planck 2018 and SH0ES around 1σ region. We compute $\ln\mathcal{B}$, ΔAIC and ΔBIC of the Mulin model relative to the fiducial model, and find

$$\ln\mathcal{B} = 39.1411\,, \quad \Delta\text{AIC} = -90.0874\,, \quad \Delta\text{BIC} = -87.2591\,. \tag{63}$$

Therefore, the Mulin model is super-strongly preferred over the fiducial model in terms of the Bayesian evidence and the information criteria AIC, BIC (n.b. Table II).

We compare all the e^{μ} models in Fig. 12, where we present e^{μ} versus $\ln\text{DM}_\text{E}$ for all the e^{μ} models, while the model parameters take their mean values obtained from the data. We find that in all the step-like e^{μ} models, $\mu_0 \sim 50$ or 30 (fairly close to the $e^{\mu} \sim 68$ of Macquart *et al.* [32] and the $e^{\mu} \sim 69$ of the fiducial model in Eq. (17)), and $\mu_1 \sim 250$ or 220, while the transition happens around $\ln\text{DM}_\text{E} \sim 5.4$. The e^{μ} of Mulin model crosses almost all steps of μ_i, as shown in Fig. 12, and hence this linear e^{μ} model is at least a decent enough approximation of the unknown e^{μ} function. The common feature of all the e^{μ} models is that e^{μ} converges to a smaller value ($\sim \mathcal{O}(10)$) to comfort the localized FRBs at low DM_E as in the fiducial model, and then e^{μ} becomes much larger at high DM_E to shift the Hubble constant H_0. The physical picture is quite clear. On the other hand, in Table III, we also summarize the Bayesian evidences and the information criteria AIC, BIC for all the e^{μ} models relative to the fiducial model. One can easily see that M3s $\gg$ Mulin $\gg$ Mu2s $\gg$ Fiducial. All the e^{μ} models are overwhelmingly preferred over the fiducial model in terms of the Bayesian evidence and the information criteria AIC, BIC. The Hubble constants H_0 can be consistent with the ones of Planck 2018 and SH0ES in all the e^{μ} models.

V. CONCLUDING REMARKS

As is well known, Hubble tension is one of the most serious challenges in cosmology to date. So, it is of interest to measure the Hubble constant by using some new probes independent of CMB and SNIa. One of the promising probes is the fast radio bursts (FRBs), which could be useful in cosmology. In the literature, the methodology proposed by Macquart *et al.* [32] has been widely used, in which both $\mathrm{DM_{IGM}}$ and $\mathrm{DM_{host}}$ are described by probability distribution functions (PDFs). Recently, it was found that in order to obtain a Hubble constant H_0 consistent with the ones of Planck 2018 and SH0ES by using the current $\mathcal{O}(100)$ localized FRBs, an unusually large $f_{\rm IGM}$ fairly close to its upper bound 1 is required, if the narrow prior bounded by 0.5 for the parameter F in the distribution of $\mathrm{DM_{IGM}}$ was used. In fact, a small F is the key to make H_0 larger. In the present work, we consider a loose prior for the parameter F, and find an unusually low H_0 by using 125 localized FRBs. We show that the model with loose F prior is strongly preferred over the one with narrow F prior in all terms of the Bayesian evidence and the information criteria AIC, BIC. So, the great Hubble tension between FRBs, Planck 2018 and SH0ES should be taken seriously. Instead of modifying $\sigma_\Delta = Fz^{-0.5}$ in the distribution of $\mathrm{DM_{IGM}}$, here we try to find a new way out by generalizing the distribution of $\mathrm{DM_{host}}$ with varying location and scale parameters ℓ and e^μ, respectively. We find that H_0 can be consistent with the ones of Planck 2018 and SH0ES in all cases. All the Bayesian evidence and the information criteria AIC, BIC for the generalized distributions of $\mathrm{DM_{host}}$ are overwhelmingly strong.

Let us look closely. In the FRB cosmology, the combination $\Theta \propto \left(\Omega_b h^2\right) f_{\rm IGM}/H_0$ defined in Eq. (4) characterizes the degeneration between H_0, $\Omega_b h^2$ and $f_{\rm IGM}$. As is well known, $\Omega_b h^2$ as a whole can be independently constrained by using e.g. CMB or big bang nucleosynthesis (BBN). So, in order to obtain a higher Hubble constant H_0, one should adopt a larger $f_{\rm IGM}$ close to its upper bound 1 for a fixed Θ, or vice versa, if a Hubble constant H_0 from SH0ES or Planck 2018 is adopted, one can find an unusually large $f_{\rm IGM}$. Actually, this is the hidden trick in the literature. So, the real key is not $f_{\rm IGM}$ or H_0. The boss behind the curtain is Θ, the pre-factor of $\langle \mathrm{DM_{IGM}} \rangle$ in Eq. (4). One can see that Θ is correlated with the parameter F in $\sigma_\Delta = Fz^{-0.5}$ describing the distribution of $\mathrm{DM_{IGM}}$, as shown by the $\Theta - F$ contours in Figs. $1-7$ and $9-11$. In order to obtain a small Θ leading to a large H_0 with a normal $f_{\rm IGM} \sim 0.83$, a small F is required. So far, we can understand the hidden secret to bound the parameter F with a small value of 0.5 (at least $F < 1$) in the literature. But we consider that it is a trick more than a physical solution. So, we have tried a new way out in the present work.

The physics in this work is $\mathrm{DM_{host}}$. As shown in Secs. III and IV, the location parameter $\ell > 0$ and/or the larger scale parameter e^μ can shift $\mathrm{DM_{host}}$ toward higher values, or equivalently, shift $\mathrm{DM_{IGM}}$ toward smaller values for the fixed $\mathrm{DM}_{\mathrm{E},\,i}$ of a given localized FRB at redshift z_i (n.b. Eq. (3)). This leads to a smaller mean $\langle \mathrm{DM_{IGM}} \rangle$, so that we find a smaller Θ as the pre-factor of $\langle \mathrm{DM_{IGM}} \rangle$, and then a larger H_0 for a normal $f_{\rm IGM} \sim 0.83$ (n.b. $\Theta \propto \left(\Omega_b h^2\right) f_{\rm IGM}/H_0$ defined in Eq. (4)). The key is Θ and $\mathrm{DM_{host}}$. Everything is natural and reasonable in this physical picture.

In this work, we have considered eight models of the generalized distributions of $\mathrm{DM_{host}}$. In Table III, we summarize the Bayesian evidences and the information criteria AIC, BIC for all models. We can easily see that Loc3s0 $>$ Loc3s $\gg$ Mu3s $\sim$ Loclin $\gg$ Mulin $\sim$ Loc2s0 $>$ Loc2s $\gg$ Mu2s $\gg$ Fiducial $\gg$ NarrowF. All the generalized $\mathrm{DM_{host}}$ models are overwhelmingly preferred over the fiducial model. We consider that the simple Loc2s0, Mu2s, Mulin or Loclin models are enough in practice.

Some open issues are left to the future. In this work, we have used the location and scale parameters ℓ and e^μ separately. But actually they could be used together, and their chemical reaction might be quite interesting. On the other hand, it is of interest to find some reasonable analytic functions for ℓ and e^μ, rather than the simple Taylor expansions considered in this work. It might be hard but worth to try in the future. Note that in e.g. [105], e^μ at redshifts 0.1, 0.2, 0.3, 0.4, 0.5, 0.7, 1.0, 1.5 have been derived from the IllustrisTNG simulation for various types of FRBs, and these e^μ monotonously become larger as redshift increases, as shown by Table 3 of [105]. This also supports a varying e^μ, and might help us to find some suitable analytic functions for e^μ. Of course, it is also interesting to explore other ways out, for example, the generalized distributions of $\mathrm{DM_{IGM}}$. Note that in e.g. [37], a new σ_Δ has been proposed to replace $\sigma_\Delta = Fz^{-0.5}$ in the distribution of $\mathrm{DM_{IGM}}$. We leave them to the future works.

ACKNOWLEDGEMENTS

We are grateful to Profs. Puxun Wu, Fa-Yin Wang, Jun-Jie Wei, Hai-Nan Lin, as well as Dao-Hong Gao, Jia-Lei Niu, Shu-Yan Long, Hui-Qiang Liu, Wei-Zhi Gong and Shuo-Yu Zhang for kind help and useful discussions. This work was supported in part by NSFC under Grants No. 12375042 and No. 11975046.

[1] E. Di Valentino *et al.*, Phys. Dark Univ. **49**, 101965 (2025) [arXiv:2504.01669].
[2] E. Abdalla *et al.*, JHEAp **34**, 49 (2022) [arXiv:2203.06142].
[3] R. G. Cai, L. Li and S. J. Wang, Acta Phys. Sin. **72**, no.23, 239801 (2023).
[4] N. Aghanim *et al.*, Astron. Astrophys. **641**, A6 (2020) [arXiv:1807.06209].
[5] A. G. Riess *et al.*, Astrophys. J. Lett. **934**, no.1, L7 (2022) [arXiv:2112.04510].
[6] https://www.nature.com/collections/rswtktxcln
[7] D. R. Lorimer, Nat. Astron. **2**, 860 (2018) [arXiv:1811.00195].
[8] E. F. Keane, Nat. Astron. **2**, 865 (2018) [arXiv:1811.00899].
[9] E. Petroff, J. W. T. Hessels and D. R. Lorimer, Astron. Astrophys. Rev. **30**, 2 (2022) [arXiv:2107.10113].
[10] D. Xiao, F. Y. Wang and Z. G. Dai, Sci. China Phys. Mech. Astron. **64**, 249501 (2021) [arXiv:2101.04907].
[11] B. Zhang, Nature **587**, 45 (2020) [arXiv:2011.03500].
[12] B. Zhang, Rev. Mod. Phys. **95**, 035005 (2023) [arXiv:2212.03972].
[13] L. Nicastro *et al.*, Universe **7**, no.3, 76 (2021) [arXiv:2103.07786].
[14] W. Deng and B. Zhang, Astrophys. J. **783**, L35 (2014) [arXiv:1401.0059].
[15] Y. P. Yang and B. Zhang, Astrophys. J. **830**, no. 2, L31 (2016) [arXiv:1608.08154].
[16] H. Gao, Z. Li and B. Zhang, Astrophys. J. **788**, 189 (2014) [arXiv:1402.2498].
[17] B. Zhou, X. Li, T. Wang, Y. Z. Fan and D. M. Wei, Phys. Rev. D **89**, 107303 (2014) [arXiv:1401.2927].
[18] D. C. Qiang, H. K. Deng and H. Wei, Class. Quant. Grav. **37**, 185022 (2020) [arXiv:1902.03580].
[19] D. C. Qiang and H. Wei, JCAP **2004**, 023 (2020) [arXiv:2002.10189].
[20] D. C. Qiang and H. Wei, Phys. Rev. D **103**, 083536 (2021) [arXiv:2102.00579].
[21] D. C. Qiang, S. L. Li and H. Wei, JCAP **2201**, 040 (2022) [arXiv:2111.07476].
[22] H. Y. Guo and H. Wei, JCAP **2207**, 010 (2022) [arXiv:2203.12551].
[23] H. Y. Guo and H. Wei, Phys. Lett. B **859**, 139120 (2024) [arXiv:2301.08194].
[24] L. Y. Li, J. Y. Jia, D. C. Qiang and H. Wei, JHEAp **49**, 100443 (2026) [arXiv:2408.12983].
[25] D. C. Qiang, Z. You, S. Yang, Z. H. Zhu and T. W. Chen, Astrophys. J. **979**, 95 (2025) [arXiv:2411.13973].
[26] D. C. Qiang, J. Zheng, Z. Q. You and S. Yang, Astrophys. J. **982**, 16 (2025) [arXiv:2411.14040].
[27] Z. W. Zhao, J. G. Zhang, Y. Li, J. F. Zhang and X. Zhang, arXiv:2212.13433 [astro-ph.CO].
[28] M. McQuinn, Astrophys. J. **780**, L33 (2014) [arXiv:1309.4451].
[29] K. Ioka, Astrophys. J. **598**, L79 (2003) [astro-ph/0309200].
[30] S. Inoue, Mon. Not. Roy. Astron. Soc. **348**, 999 (2004) [astro-ph/0309364].
[31] M. Jaroszynski, Mon. Not. Roy. Astron. Soc. **484**, no. 2, 1637 (2019) [arXiv:1812.11936].
[32] J. P. Macquart *et al.* Nature **581**, no.7809, 391 (2020) [arXiv:2005.13161].
[33] Q. Wu, G. Q. Zhang and F. Y. Wang, Mon. Not. Roy. Astron. Soc. **515**, L1 (2022) [arXiv:2108.00581].
[34] S. Kalita, S. Bhatporia and A. Weltman, Phys. Dark Univ. **48**, 101926 (2025) [arXiv:2410.01974].
[35] D. H. Gao *et al.*, Astron. Astrophys. **698**, A215 (2025) [arXiv:2410.03994].
[36] T. Lemos, arXiv:2507.17693 [astro-ph.CO].
[37] J. Zhuge, M. Kalomenopoulos and B. Zhang, arXiv:2508.05161 [astro-ph.CO].
[38] J. Baptista *et al.*, Astrophys. J. **965**, no.1, 57 (2024) [arXiv:2305.07022].
[39] C. Xu, Y. Feng and J. Xu, Astrophys. J. **988**, no.2, 177 (2025) [arXiv:2507.18946].
[40] J. M. Cordes and T. J. W. Lazio, astro-ph/0207156.
[41] J. M. Cordes and T. J. W. Lazio, astro-ph/0301598.
[42] S. Yamasaki and T. Totani, Astrophys. J. **888**, no.2, 105 (2020) [arXiv:1909.00849].
[43] https://pypi.org/project/pygedm and https://pygedm.readthedocs.io
[44] D. C. Price, C. Flynn and A. Deller, Publ. Astron. Soc. Austral. **38**, e038 (2021) [arXiv:2106.15816].
[45] https://docs.scipy.org/doc/scipy/reference/generated/scipy.stats.lognorm.html
[46] https://github.com/FRBs/FRB
[47] Y. Zhang, Y. Liu, H. Yu and P. Wu, arXiv:2504.06845 [astro-ph.CO].
[48] Y. Liu, Y. Zhang, H. Yu and P. Wu, arXiv:2506.03536 [astro-ph.CO].
[49] J. Torrado and A. Lewis, JCAP **2105**, 057 (2021) [arXiv:2005.05290].
[50] https://cobaya.readthedocs.org
[51] A. Lewis, arXiv:1910.13970 [astro-ph.IM].
[52] https://getdist.readthedocs.io
[53] C. H. Niu *et al.*, Nature **606**, no.7916, 873 (2022) [arXiv:2110.07418].
[54] L. Connor *et al.*, Nature Astron. **9**, no.8, 1226 (2025) [arXiv:2409.16952].
[55] K. G. Lee *et al.*, Astrophys. J. Lett. **954**, no.1, L7 (2023) [arXiv:2306.05403].
[56] C. J. Law *et al.*, Astrophys. J. **967**, no.1, 29 (2024) [arXiv:2307.03344].
[57] K. Sharma *et al.*, Nature **635**, no.8037, 61 (2024) [arXiv:2409.16964].

[58] V. Ravi *et al.*, Astrophys. J. Lett. **949**, no.1, L3 (2023) [arXiv:2211.09049].
[59] Y. K. Zhang *et al.*, Astrophys. J. **955**, no.2, 142 (2023) [arXiv:2304.14665].
[60] S. Bhandari *et al.*, Astrophys. J. **948**, no.1, 67 (2023) [arXiv:2211.16790].
[61] M. Bhardwaj *et al.*, Astrophys. J. Lett. **971**, no.2, L51 (2024) [arXiv:2310.10018].
[62] M. Amiri *et al.*, Astrophys. J. Supp. **257**, no.2, 59 (2021) [arXiv:2106.04352].
[63] S. D. Ryder *et al.*, Science **392**, 294 (2023) [arXiv:2210.04680].
[64] M. Bhardwaj *et al.*, Astrophys. J. Lett. **910**, no.2, L18 (2021) [arXiv:2103.01295].
[65] E. K. Mahony *et al.*, Astrophys. J. Lett. **867**, no.1, L10 (2018) [arXiv:1810.04354].
[66] A. C. Gordon *et al.*, Astrophys. J. **954**, no.1, 80 (2023) [arXiv:2302.05465].
[67] D. C. Price *et al.*, Mon. Not. Roy. Astron. Soc. **486**, no.3, 3636 (2019) [arXiv:1901.07412].
[68] D. Hiramatsu *et al.*, Astrophys. J. Lett. **947**, no.2, L28 (2023) [arXiv:2211.03974].
[69] J. O. Chibueze *et al.*, Mon. Not. Roy. Astron. Soc. **515**, no.1, 1365 (2022) [arXiv:2201.00069].
[70] C. Guidorzi *et al.*, Astron. Astrophys. **637**, A69 (2020) [arXiv:2003.10889].
[71] S. Bhandari *et al.*, Astrophys. J. Lett. **901**, no.2, L20 (2020) [arXiv:2008.12488].
[72] A. E. Lanman *et al.*, Astrophys. J. **927**, no.1, 59 (2022) [arXiv:2109.09254].
[73] M. Caleb *et al.*, Mon. Not. Roy. Astron. Soc. **524**, no.2, 2064 (2023) [arXiv:2302.09754].
[74] A. L. Ibik *et al.*, Astrophys. J. **961**, no.1, 99 (2024) [arXiv:2304.02638].
[75] D. Michilli *et al.*, Astrophys. J. **950**, no.2, 134 (2023) [arXiv:2212.11941].
[76] L. N. Driessen *et al.*, Mon. Not. Roy. Astron. Soc. **527**, no.2, 3659 (2023) [arXiv:2302.09787].
[77] S. Bhandari *et al.*, Astron. J. **163**, no.2, 69 (2022) [arXiv:2108.01282].
[78] M. Bhardwaj *et al.*, Astrophys. J. Lett. **919**, no.2, L24 (2021) [arXiv:2108.12122].
[79] V. Ravi *et al.*, Nature **572**, no.7769, 352 (2019) [arXiv:1907.01542].
[80] C. J. Law *et al.*, Astrophys. J. **899**, no.2, 161 (2020) [arXiv:2007.02155].
[81] T. Cassanelli *et al.*, Nature Astron. **8**, no.11, 1429 (2024) [arXiv:2307.09502].
[82] J. Tian *et al.*, Mon. Not. Roy. Astron. Soc. **533**, no.3, 3174 (2024) [arXiv:2408.10988].
[83] R. M. Shannon *et al.*, Publ. Astron. Soc. Austral. **42**, e036 (2025) [arXiv:2408.02083].
[84] W. R. Arcus *et al.*, Publ. Astron. Soc. Austral. **42**, e003 (2025) [arXiv:2408.09351].
[85] M. Glowacki *et al.*, Astrophys. J. Lett. **962**, no.1, L13 (2024) [arXiv:2311.16808].
[86] K. M. Rajwade *et al.*, Mon. Not. Roy. Astron. Soc. **514**, no.2, 1961 (2022) [arXiv:2205.14600].
[87] S. Kalita, Mon. Not. Roy. Astron. Soc. **533**, no.1, L57 (2024) [arXiv:2407.01736].
[88] M. Amiri *et al.*, Astrophys. J. Suppl. **280**, no.1, 6 (2025) [arXiv:2502.11217].
[89] Y. Y. Wang, S. J. Gao and Y. Z. Fan, Astrophys. J. **981**, no.1, 9 (2025) [arXiv:2501.09260].
[90] Y. Li *et al.*, arXiv:2503.04727 [astro-ph.HE].
[91] E. F. Piratova-Moreno *et al.*, arXiv:2502.08509 [astro-ph.CO].
[92] I. Pastor-Marazuela *et al.*, arXiv:2507.05982 [astro-ph.HE].
[93] M. Caleb *et al.*, arXiv:2508.01648 [astro-ph.HE].
[94] T. C. Abbott *et al.*, Astrophys. J. Lett. **989**, no.2, L48 (2025) [arXiv:2506.19006].
[95] A. Curtin *et al.*, arXiv:2506.10961 [astro-ph.HE].
[96] L. Perivolaropoulos and F. Skara, Universe **8**, no.10, 502 (2022) [arXiv:2208.11169].
[97] M. Kilbinger *et al.*, Mon. Not. Roy. Astron. Soc. **405**, 2381 (2010) [arXiv:0912.1614].
[98] A. Heavens *et al.*, Phys. Rev. Lett. **119**, no.10, 101301 (2017) [arXiv:1704.03467].
[99] J. Y. Jia, J. L. Niu, D. C. Qiang and H. Wei, Phys. Rev. D **112**, 043507 (2025) [arXiv:2504.13380].
[100] A. Heavens *et al.*, arXiv:1704.03472 [stat.CO].
[101] https://github.com/yabebalFantaye/MCEvidence
[102] https://github.com/BorisNgHL/MCEvi_mod
[103] H. Akaike, IEEE Trans. Automatic Control **19**, 716 (1974).
[104] G. Schwarz, Ann. Stat. **6**, 461 (1978).
[105] G. Q. Zhang, H. Yu, J. H. He and F. Y. Wang, Astrophys. J. **900**, no.2, 170 (2020) [arXiv:2007.13935].